NTNU – Trondheim
Norwegian University of
Science and Technology

Estimation of Formation Water rate using Unscented Kalman filtering with application to the Snøhvit Gas/Condensate Field.

Anders Jordtveit Mørk

Master of Science in Engineering Cybernetics
Submission date: June 2013
Supervisor: Lars Imsland, ITK

Norwegian University of Science and Technology
Department of Engineering Cybernetics

NTNU

Faculty of Information Technology, Mathematics and Electrical Engineering
Department of Engineering Cybernetics

PROJECT DESCRIPTION SHEET

Name of the candidate: Anders Jordtveit Mørk

Thesis title (English): Estimation of formation water rate using unscented Kalman filtering with application to the Snøhvit gas/condensate field.

Background

Snøhvit is a gas/condensate field and is the world's most northerly offshore field, located at 70 degrees north. The field is at a sea-depth of 300 m and every day 20.8 MSm3 of natural gas is transported through the 143 km long multiphase pipeline to Melkøya in Hammerfest. At the seabed, MEG is continuously injected into the gas/condensate to prevent hydrate formation. At Melkøya, the gas, condensate and MEG/Water are separated and MEG is regenerated from MEG/Water and re-injected into the gas/condensate stream at the seabed. The gas is further processed into LNG and LPG, and together with the condensate, they are all products that are transported using specialized tankers to the marked in Sothern Europe and USA.

Determining produced formation water rate from the gas/condensate reservoir is important due to sometimes limited onshore desalination capacity and enhanced scale potential caused by the salty water. At the Snøhvit field, the produced formation water will accumulate in the MEG loop, and may precipitate at unwanted locations once it exceeds the solubility limits of the various salts.

This Master project is given by Statoil, and is an independent follow-up of project work fall 2012.

Work description

The following tasks should be conducted as part of the master thesis work:

1. Establish a dynamic model (simplified) for the MEG loop.
2. Perform response analysis using the dynamic model and compare the model response with real production data.
3. Implement an unscented Kalman filter to dynamically estimate the total rate of produced formation water

Start date: 14. January, 2013 **Due date:** 10. June, 2013

Supervisor: Lars Imsland
Co-advisor(s): Geir Arne Evjen, Statoil

Trondheim, __21.01.2013_____

Lars Imsland
Supervisor

Address
Sem Sælandsvei 5
NO-7491 Trondheim

Org.no. 974 767 880
E-mail:
postmottak@itk.ntnu.no
http://www.itk.ntnu.no

Location
O.S. Bragstads plass 2D
NO-7034 Trondheim

Phone
+ 47 73 59 43 76
Fax
+ 47 73 59 45 99

Phone: + 47 47 23 19 49

Abstract

In this thesis, a simplified model of the MEG loop at the Snøhvit field is established and implemented, together with an unscented Kalman filter. The model is tested with and without the Kalman filter. The model is tested with test data, while the model included the Kalman filter is tested with both test data and real production data.

It is found that the model is some part away from the real process. The most significant difference is the rate of rich MEG into the MEG-regenerator onshore, which in the real process has severe oscillations relative to the rate of lean MEG rate out of the MEG-regenerator. In the model the rich MEG is modeled primarily to follow the lean MEG rate, and is therefore fairly constant.

For many data sets of real production data, the system is not able to predict the formation water, because the error covariance matrix in the Kalman filter becomes negative semi definite. This can be caused by the Kalman filter not being robust enough or/and inconsistent data from Snøhvit. Still, when a data set is found where the system is able to predict the formation water is found, the system does predict a formation water rate that is located in the region that is expected at the Snøhvit field.

Sammendrag

I denne avhandlingen blir en forenklet model av MEG sløyfen på Snøhvit-feltet utviklet og implementert sammen med et unscented Kalmanfilter. Modellen er testet med og uten Kalmanfilteret. Modellen er testet med prøvedata, mens modellen, sammen med Kalmanfilteret, er testet både med prøvedata og ekte produksjonsdata.

Det er vist at modellen ikke er helt lik den ekte prosessen. Den største forskjellen er at rik MEG raten in i MEG-regeneratoren har store oscillasjoner i den ekte prosessen i forhold til lean MEG raten ut av MEG-regeneratoren. I modellen er rik MEG raten hovedsaklig modellert til å følge lean MEG raten, og er derfor ganske konstant.

For mange datasett av ekte produksjonsdata er ikke ikke mulig for systemet å predikere produsert formasjonsvann, siden feilvarians-matrisen i Kalmanfilteret blir negativ semidefinitt. Dette kan være forårsaket av at Kalmanfilteret ikke er robus nok og/eller inkonsistente data fra Snøhvit. Men når et datasett hvor system klarer å gjennomføre prediksjonene av formasjonsvannet er funnet, klarer systemet å prediktere en formasjonsvann-rate som ligger i det området som er forventet av produsert formasjonsvann fra Snøhvit-feltet.

Preface

This report is the master thesis produced in the course TTK4900, Engineering Cybernetics, Master Thesis. The thesis is the final part of my study at the Norwegian University of Technology and Science (NTNU) and concludes my 5 years at NTNU. The thesis is a continuation of my project work, conducted in the course TTK4550, Project Specialization, and is a thesis done in for Statoil AS.

I would like to thank my supervisor at NTNU, Lars Imsland, who has guided me through the thesis, especially with the parts concerning the Kalman filter. Further I would like to thank Geir Arne Evjen, representing Statoil, who has been my co-advisor in this thesis. He has helped me with practical issues, including gathering data from Statoil, granting access to different documents and software from Statoil etc. He has also been very helpful in explaining how the process works.

At last I will thank my fellow students whom I have shared office with the last year. They are Mikael Berg, Håvard Håkon Raaen, Torstein Thode Kristoffersen, Henrik Emil Wold, Mikkel Solberg and Tone Ljones. All of them have been helpful in discussing my thesis and contributing to several humorous moments during this semester.

Anders Jordtveit Mørk
June 2013, Trondheim

Contents

List of Figures

List of Tables

Nomenclature

APE	Aspen Process Explorer
CDU	Control Distrubution Unit
CF	Completion Fluid
EKF	Extended Kalman Filter
FW	Formation Water
LM	Lean MEG
LNG	Liquified Natural Gas
MEG	Mono-Ethylene-Glycol
NGL	Natural Gas Liquids
RM	Rich MEG
SW	Sea Water
UKF	Unscented Kalman Filter
w%	Weight percent

Chapter 1

Introduction

This master thesis, TTK4900, is a continuation of the project done in the course TTK4550, Specialization project. In that project the main focus was to understand the process and to understand the data reconciliation method used to solve the process. A simplified version of the data reconciliation was also implemented. For more information about the Specialization project, see [8].

In this master thesis a new approach is used to solve the system, the data reconciliation is replaced with an unscented Kalman filter. In the project the process where the estimating was conducted, was the process at the Vega field, while in this master thesis the process in question is the Snøhvit field. These two fields are quite similar, but with some differences.

1.1 Snøhvit

The first well drilled to search for hydrocarbons in the North Sea was drilled on the summer of 1966. The well was dry, but three years later, in 1969, it was found an oil field in the North Sea. That field was the Ekofisk field, and the production was started 15. June 1971. In the following years several large findings were discovered. In 1972 the Norwegian state-owned company Statoil AS was founded to make sure Norwegian participation in the north sea was ensured [11].

The following paragraph contains information about the Snøhvit field that is obtained from [1]. The Snøhvit field is located in the Norwegian sea (often called the Barents sea in relation to petroleum industry [10]) northwest of Hammerfest, and is the first field that is developed in the Barents Sea. Snøhvit is also the first field on the Norwegian continental shelf without any installations on the sea surface. The production plant is located on the seabed between 250 and 345 meter beneath the surface.

The field produces gas, and it is planned to be drilled twenty wells, distributed between the three reservoirs Snøhvit, Albatross and Askeladd. The gas is transported in a 143 km long pipeline from the seabed to Melkøya, outside Hammerfest. The Snøhvit reservoir consists of eight wells in addition to one well for CO_2-

injection. The Albatross reservoir contains four wells, while the Askeladd reservoir consists of eight wells [10]. The CO_2 content is separated at Melkøya and re-injected into the field [12].

The Snøhvit field was proven in 1984 [10]. The start of the production on the Snøhvit field took place on 21. August 2007, where both the Snøhvit and the Albatross reservoirs were taken into use. The Askeladd reservoir is scheduled to start it's production in the year 2014/2015.

Figure 1.1: The onshore process plant at Melkøya outside of Hammerfest. The production from this process plant started 13. September 2007. The picture is obtained from [1], and the photographer is Gjertrud Lindberg.

The Snøhvit field is operated by Statoil, which is the biggest partner with about 37 % of the ownership of the field. The second highest owner of the field is Petoro with about 30 % of the ownership. The field is predicted, per 31. December 2012, to contain 176.6 billion[1] Sm^3 gas, 6.4 million tons NGL (natural gas liquids) and 22.6 million Sm^3 condensate. Per 31. December 2012 there is predicted to be 156.9 billion tons Sm^3 remaining gas [12].

1.2 Problem objectives

The work description given for this master thesis consists of the following three objectives:

1. Establish a dynamic model (simplified) for the MEG loop.

[1] 1 billion = 1 000 000 000. In Norwegian: *milliard*.

2. Perform response analysis using the dynamic model and compare the model response with real production data.

3. Implement an unscented Kalman filter to dynamically estimate the total rate of produced formation water.

The first objective is to establish a dynamic model to describe the MEG loop at the Snøhvit field. The model implemented will be a simplification of the real system, due to the complexity of the real system. A more complex model will also lead to more complexity of making the Kalman filter work. Therefore the main focus when establishing the model is to include the most essential dynamics of the real system.

The second objective is to perform response analysis using the dynamic model and compare the model response with real production data. This objective will be a bit more extensive than expressed in the description. The model will be tested with sample data, to test if the model works as expected. Then the model together with the Kalman filter will be tested with sample data to see if the Kalman filter is working properly. Then the model with Kalman filter will be tested with production data, to see how the implemented system will function when production data is applied.

The last objective is to implement the unscented Kalman filter, with focus on estimating the total rate of produced formation water. The implementation of the Kalman filter also includes some important aspects as tuning of the Kalman filter and introduction of constraints on the states.

1.3 Outline and scope

The main tasks that will be performed in this thesis are listed in the table below:

- Develop and implementation of a dynamic model of the system.
- Implementation of an unscented Kalman filter.
- Stability analysis of the system.
- Testing of the dynamic model.
- Tuning of the unscented Kalman filter.
- Testing of model with the unscented Kalman filter.
- Testing of model with the unscented Kalman filter with real production data.

This thesis will, after the introduction first contain a part that describe the process more detailed than done in this chapter. This is done in Chapter 2, The MEG process. Some parts of this chapter is re-used from the project [8]. Then the model development of the process will be described in Chapter 3, Model development, and the discretization of the model, with an analysis of the numerical

solver, will be done in the chapter after, Chapter 4, Numerical solver and model discretization.

Then there will be a theory part, Chapter 5, Kalman filter. In this part, the Kalman filter and the unscented Kalman filter will be described.

Further the more practical part of this thesis will come. The first chapter in this part is Chapter 6, Model implementation, that describes the model implementation of the model. Further the tuning of the Kalman filter will appear in Chapter 7, Tuning.

In Chapter 8, Results, the results of the simulations done in this thesis will be displayed.

The thesis will be concluded with a chapter, Chapter 9, Discussion, that will discuss the results found in this thesis. Further some conclusions and proposals to further work is given in Chapter 10, Conclusion and further work.

After the table of contents a list of figures, a list of tables and the nomenclature are listed. In the appendix, after the references, a list explaining the notation and a list of symbols used in this thesis are displayed.

1.4 Motivation

At several of Statoils process plants there are implemented a software named Megsim. Megsim is a software that is monitoring and predicting different variables of the process. The software is quite similar for each of the fields, but there are some variations due to variations of the production process at the different fields. Therefore Megsim is implemented individually for each field. At the Vega field the software version is called Megsim Vega, while at the Snøhvit field the software version will be called Megsim Snøhvit.

The method that is currently used in Megsim to monitor the process is data reconciliation and gross error detection. Statoil has experienced some difficulties with Megsim for the different fields, like the Vega field. This is because the software has experienced periods when it has been unable to perform the data reconciliation. As a result the measurements and the estimates have been unavailable for the user of the software to obtain. In the beginning some form of Kalman filter was tested in Megsim, but the attempt was unsuccessful, probably due to the large amount of variables that was taken into account and the amount of variables tried to predict.

At Snøhvit, Statoil is in the process of implementing a new addition of Megsim, designed for the Snøhvit field. Statoil is mainly planning to use the same approach as done earlier with data reconciliation and gross error detection, but they also want to try another implementation of a Kalman filter. The new approach of the Kalman filter, which will be performed in this master thesis, will not be as extensive as Statoils earlier attempt. Therefore the main goal of the Kalman filter will be to just predict the most crucial state of the system, the formation water rate from the reservoirs. If this is successful, the model can be expanded and be done more extensive, with more parameters to predict.

If the prediction of the formation water rate, and other system parameters, is successful, Statoil can optimize the use of inhibitors and pH-stabilizer. This will

make the process more effective in hence of waste products and costs.

Chapter 2

The MEG process

The process plant at Melkøya is a liquid natural gas (LNG) plant for producing and distributing gas from the Snøhvit field. In this chapter it will be focused on the part of the system that is important for this thesis, which includes the MEG loop and the different fluids that are part of that loop. That means it will not be used any time on explaining the other parts of the LNG production at Melkøya.

2.1 The MEG loop

The MEG loop is the part of the process that is relevant for the transportation of MEG. In this section the MEG loop will be divided into two parts when explained. That is the part of the MEG loop which is offshore and the part of the MEG loop which is onshore at Melkøya. A simplified illustration of the MEG loop is shown in Figure 2.1. But first the MEG will be introduced.

2.1.1 Mono-ethylene glycol

Mono-ethylene glycol (MEG), or just ethylene glycol, is the liquid that has given its name to the MEG loop. In processes of extracting natural gases MEG is used to extract water. More importantly it prevents formation of hydrates and it also counteracts against water freezing in the pipelines [8]. The largest area of application for MEG is probably as a antifreeze fluid to vehicle engines [3].

The reservoir is a gas/condensate reservoir that is saturated with water. The water which is in the gas is not desired, due to hydrate formation. Therefore the water is extracted from the gas with MEG. This happens because the vapor pressure of water is lowered by the MEG, and water drops out and forms MEG/water phase.

In this process, MEG is separated in two types, lean MEG and rich MEG. The lean MEG is transported down to the wells by the injection lines, while the rich MEG is a part of the contents in the production line. The lean MEG contains low amounts of water, while the rich MEG contains higher amounts of water. Typical

values for the rich MEG is about 50-60 $wt\%$ MEG and the lean MEG consists of about 90 $wt\%$ MEG.

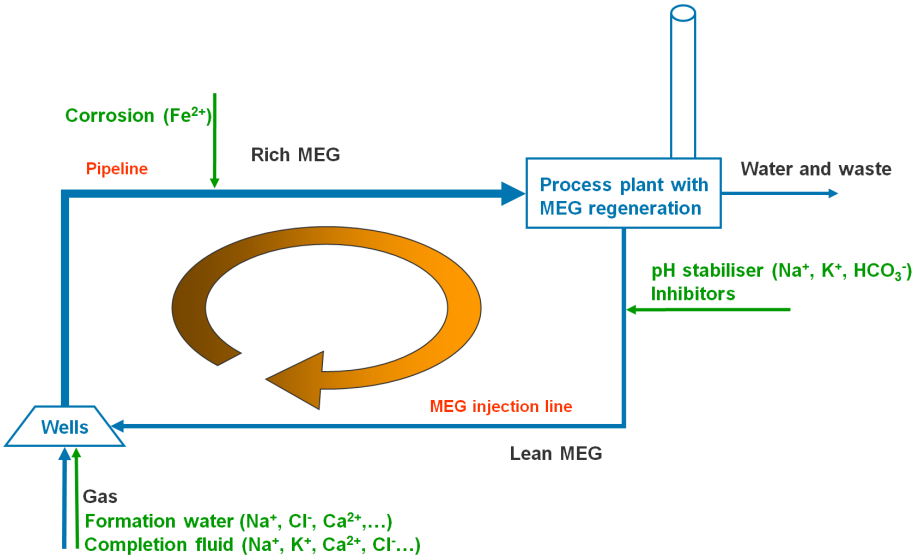

Figure 2.1: A simplified figure of the MEG loop at the Snøhvit field. The figure is used with permission from Statoil.

2.1.2 The MEG loop offshore

The connection between the wells at the Snøhvit field and the process plant at Melkøya is two 143 km long pipelines. The main pipeline, called the production line, transports the gas from the wells together with the rich MEG and condensate to Melkøya. The other pipeline is the injection line. The injection line transports lean MEG down to the wells from Melkøya.

At the wells the lean MEG from the injection line is injected into the produced fluids from the reservoirs. The lean MEG is sent to the CDU (control distribution unit) where the MEG is distributed to each of the wellheads. There are currently two operating reservoirs at the Snøhvit field, that is the Albatross reservoir and the Snøhvit reservoir, with a combined number of wells of twelve.

In every well the MEG is mixed with gas and sent up with the production line. The production fluid is cooled down since the production pipeline is submerged in seawater. The MEG extracts water from the gas in the production pipeline, therefore the MEG consists of more water than it had in the production line, and is called rich MEG.

2.1.3 The MEG loop at Melkøya

The onshore plant, which is located at Melkøya, consists of many elements. For the MEG loop, the desalination plant and the MEG-regenerator plant is the most essential parts. The first part of the extraction of the gas, called slug catcher, separates the condensate, the gas and the MEG/water phase into three different mass flows. The only essential flow out of the slug catcher, for this thesis, is the MEG/water phase. The MEG/water phase is the same as the rich MEG flow.

Some of the MEG/water phase is sent through a desalination plant after the slug catcher. The MEG/water phase flow goes further to a separation column tank. From the separation column it is extracted a mass flow of water which contains salts, and removed from the system. After the separation column the MEG/water phase is sent to the MEG-regenerator.

The MEG-regeneration tank

The MEG-regeneration tank is also referred to as the MEG-recycler in this thesis. The MEG-regeneration tank consists of many different tanks. These tanks consist of both lean MEG and rich MEG with different degrees of purity with respect of water. The reason of why there are tanks with different purity is because the operators should be able to adjust the purity of lean MEG sent into the injection pipeline. Because of the bypass in the desalination plant, explained underneath, the lean MEG is not completely cleansed for salts and consists of small amounts of salts when it is sent into the injection pipeline. This phenomenon is called carry over [8].

The desalination plant

Before the contents of the production line reach the MEG-regenerator, it is desalinated in the desalination plant. The desalination plant is a salt removal unit where salts from the rich MEG are removed before it is injected into the MEG-regenerator. The unit is needed to keep the salt level at an acceptable level. A simplified model of the desalination process is figured in Figure 2.2.

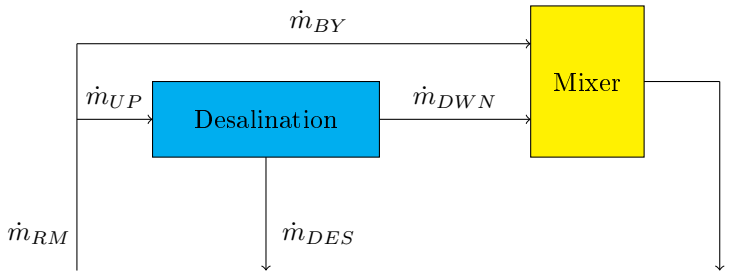

Figure 2.2: A simple chart of the desalination process.

In the desalination plant it exist one bypass pipeline, which is a pipeline that

bypasses some of the rich MEG, so that flow is not desalinated. The content that is not injected to the bypass will go through the desalination block. The waste of the desalination is solid, and all of the salts that exist in the flow through the desalination plant is removed. The mass flow through the desalination plant and the mass flow through the bypass i mixed mixed before they are sent to the MEG-regenerator.

2.2 Fluids in the MEG-loop

There are several different fluids in the MEG-loop. The different fluids is also explained in [8].

2.2.1 Formation water

Formation water is water contained in the reservoirs together with oil and gas. When extracting oil and gas, some of the formation water will be extracted as well. The formation water consist of several different minerals and salts, which makes it possible to detect the formation water and distinguish it from other types of water, like sea water, since the concentrations of ions of these waters differ significantly.

The formation water is, when produced and mixed with the pH-stabilizer, the main reason scale inside the pipelines is produced [8]. It is expected to be small amounts of formation water produced in the start of the field's lifetime, and it will increase as the time goes on. At Snøhvit, which is a young field, it is expected to bee almost zero formation water produced at this stage. The formation water at Snøhvit is expected to be produced around year 2018. It varies from field to field when in the field's lifetime the formation water is produced.

2.2.2 PH-stabilizer

PH-stabilizer is injected continuously to control the pH-values in the rich MEG. This is needed because there are CO_2 with the gas produced, that reduces the pH-value. It is added to the lean MEG after it is sent from the process plant. The pH-control is used to minimize the formation of corrosion products in the pipelines. The pH-stabilizer consists of 30 $wt\%$ of NaOH. In Figure 2.3b the result of corrosion in the pipelines is shown. Sometimes corrosion inhibitor is injected together with the pH-stabilizer in order to control the corrosion rate.

2.2.3 Scale inhibitor

PH-stabilizer is incompatible with formation water leading to scale (solid particles) formation. To prevent scale from forming, a chemical inhibitor, scale inhibitor, is injected. The scale inhibitor is added to the lean MEG after it is sent from the process plant. In Figure 2.3a the results of scale formation in the pipelines are shown.

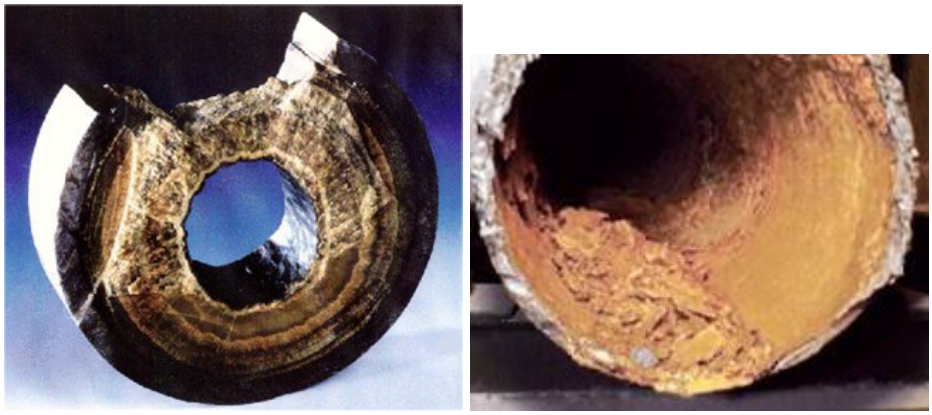

(a) (b)

Figure 2.3: Figure (a) shows scale inside the pipeline, while figure (b) shows the effect of corrosion on the pipeline. Pictures taken from [6].

2.2.4 Sea water

Before producing oil and gas from reservoirs, pipelines are submerged into the sea water, and therefore filled with sea water. After the pipelines were installed they were filled with MEG and pH-stabilizer to get rid of the sea water, but there is usually some small amounts of sea water left in the pipelines. After some days of production the amount of sea water left in the pipelines are approximately zero [8]. The sea water is also referred to as salt water.

2.2.5 Completion fluids

A completion fluid is a weight material that is used to finalize the wells when they are drilled. It will still be coming some remains of the completion fluid from the startup [8]. Together with the salt water, there are almost nothing completion fluid in the pipelines at Snøhvit.

Chapter 3

Model development

In this chapter the simplified dynamical model will be developed. This is done with basis on the process description in Chapter 2, The MEG process. First in this chapter the process is further simplified before it later is modeled. Afterwards each components of the process is described and explained more extensive.

In this chapter the model is just shown for one specie when the species are modeled. This is done since it is not any difference between the species when it comes to the modeling part. The model consists of three species.

3.1 Model simplification

In this section the process is simplified further, before the model is established in the last part of this section.

3.1.1 Simplification of the real process

The process, described in Chapter 2, is simplified to the chart displayed in Figure 3.1. In the figure, the MEG-recycler, the desalination block and the mixer represents the facilities that are onshore. The MEG-regenerator originally contains several tanks containing both lean MEG and rich MEG. The well is represented as a single well, despite the fact that the real process consists of several wells from the two reservoirs, Albatross and Snøhvit.

The time delays in the system are represented with the white blocks containing the numerical equation for transport delay, $e^{-\tau s}$. The desalination process is simplified to a desalination block that extracts salts and the mixer that mixes the bypass mass flow with the downwards mass flow from the desalination. The mixer also extracts water from the process.

The two mass flows that are produced from the well are the formation water, $\dot{m}_{FW}$, together with the condensate water that is removed from the gas, $\dot{m}_{WAT,1}$, and becomes a part of the rich MEG. The salts out from the desalination plant is

denoted by $\dot{m}_{DES}$, and the water extracted from the rich MEG is denoted with $\dot{m}_{WAT,2}$.

The flow into the MEG-recycler, $\dot{m}_{IN}$, consists of the injected chemicals, which includes the pH-stabilizer and the formation inhibitor. The refilling of MEG is not included in this figure.

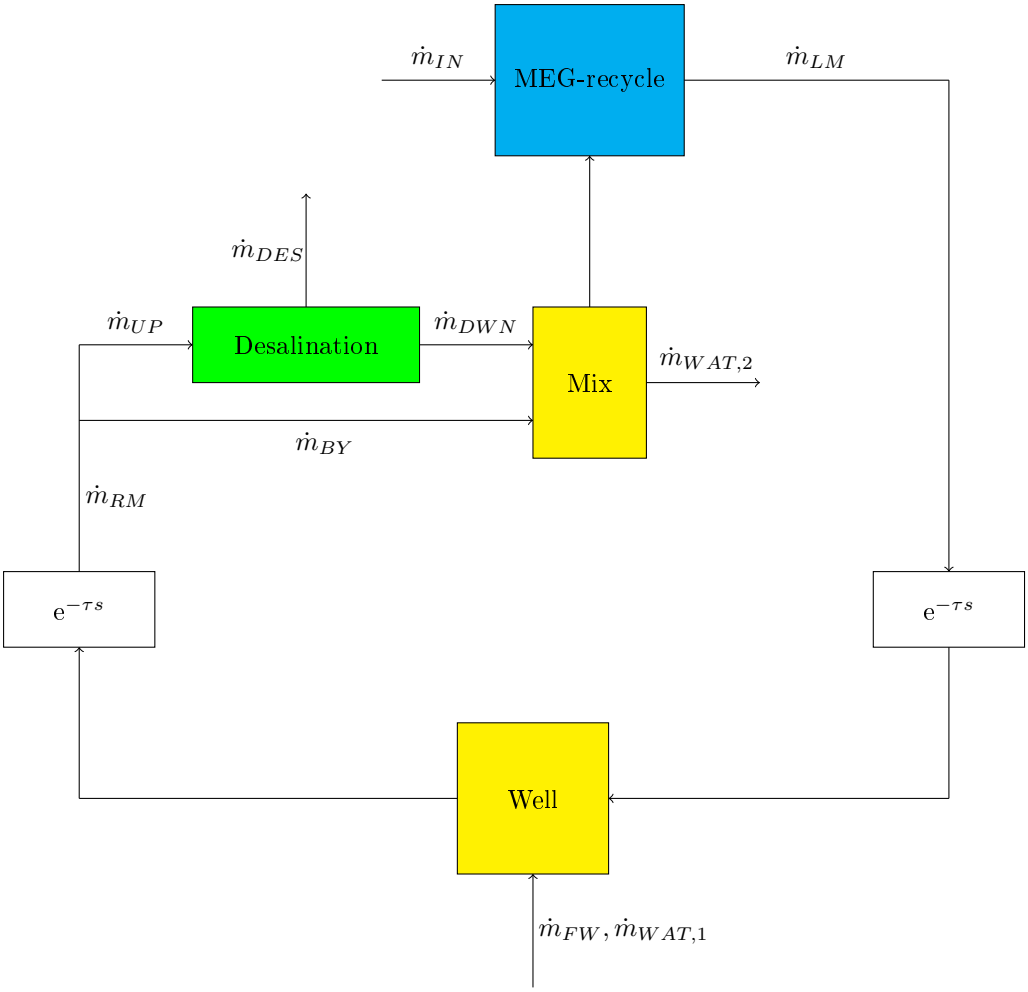

Figure 3.1: A simplified chart of the real MEG loop. The chart is shown with respect of total mass flows.

3.1.2 Model simplification

The system is modeled with respect of mass. This means the flow rates are measured as mass flows, $[kg/h]$, and the content in tanks are modeled as mass, $[kg]$. This is chosen because most of the measurements taken at Snøhvit is mass flow

rate and the amount of species in the different flows are given as concentration, $[kg/m^3]$.

In Figure 3.2 the simplified model is shown. The model, which is a further simplification of the process chart displayed in Figure 3.1, contains one tank, the MEG-recycler, and one mixer, the well. That means that both the desalination block and the mixer from Figure 3.1 is merged into the MEG-recycler.

The mixer mixes the production from the well with the lean MEG flow, the rich MEG is the output flow of the mixer. From the reservoirs, the flow rate that is of interest is the formation water, $\dot{m}_{FW}$. In this model both the mass flow of sea water and completion fluid are simplified to be zero. If this should not be the case, they will be a part of the formation water mass flow.

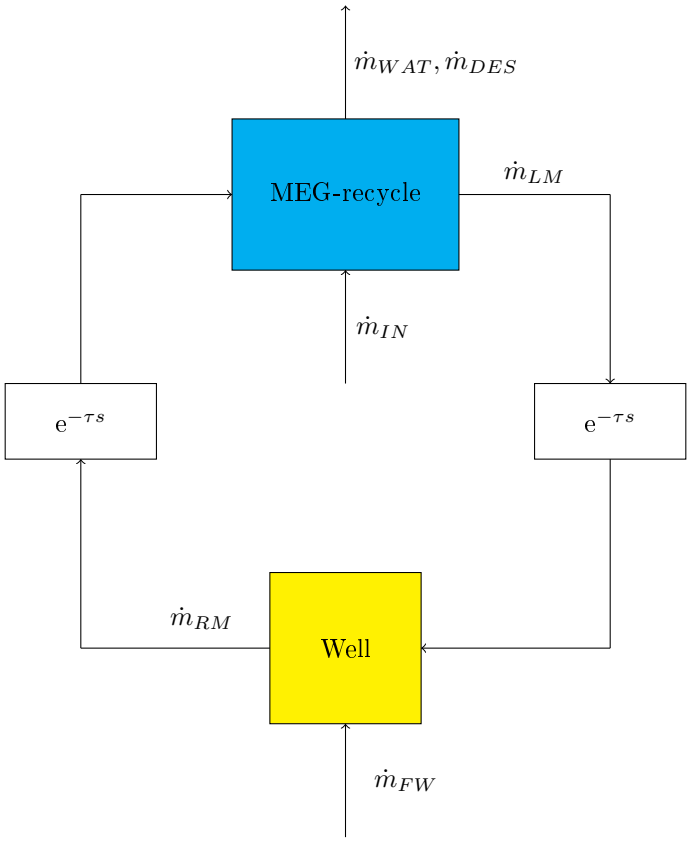

Figure 3.2: The simplified model of the Snøhvit field. The mass flows are with respect of the total mass.

The input to the MEG-recycler is the rich MEG and a flow containing the pH-stabilizer and both inhibitors, the scale inhibitor and the corrosion inhibitor, $\dot{m}_{IN}$. The output of the tank is the lean MEG flow, $\dot{m}_{LM}$, the mass flow containing the extraction of salts in the desalination plant, $\dot{m}_{DES}$, and the water extracted from

the MEG-recycler, $\dot{m}_{WAT}$. The transport delay is unchanged from the simplified process chart.

In the model the species are seen upon as inert, that means they will not react with any material, like the pH-stabilizer or the scale inhibitor. The scale inhibitor does not react with any of the species, so that assumption is true, while the pH-stabilizer may react with some of the species in the real process. Both the pH-stabilizer and the inhibitors are assumed to not include any of the relevant species.

The water extracted from the gas will not be considered as a part of the formation water, and will first be detected in the total mass flow of the rich MEG into the MEG-recycler.

3.2 The MEG-regeneration tank

The whole process from the rich MEG reach the onshore plant until it leaves the plant as lean MEG is modeled as one unit. This unit is divided into a series of many mass units to take into account the time delay that is onshore. This can also be seen upon as many tanks in series and will therefore sometimes be referred to as tanks. In Figure 3.3 an example of the MEG-recycler with four mass units is pictured. The mass units will be denoted with M_l, where l denotes for which of the mass units it yields. All external inputs and outputs to the MEG-regenerator interfere with the first mass unit.

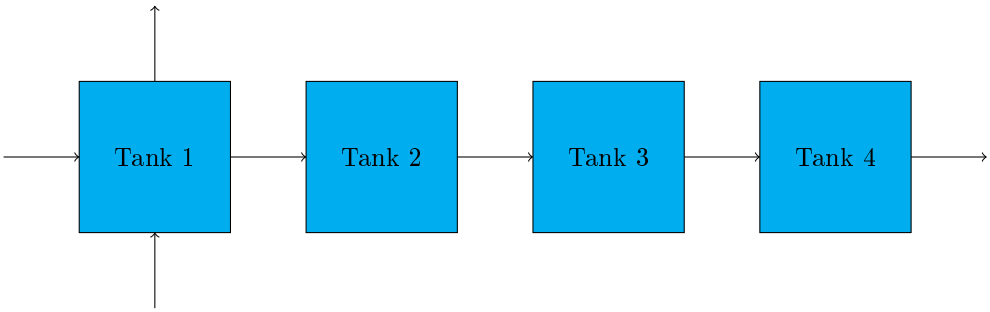

Figure 3.3: The model of the MEG-regenerator. Each tank represent each of the mass units. In this figure the MEG-recycler is modeled as four mass units.

First the change of the mass, $\frac{dM_l^i}{dt}$, of each specie i in the mass units are derived. In equations (3.3-3.5) is an example of three mass units in the MEG-recycler is described. The mass flow out of the first tank and into the second tank is denoted with $\dot{m}_1$. The same yields between the other tanks. The mass flow of each specie between the tanks, $\dot{m}_j^i$ is set to be the same ratio with the total mass flow between the tanks, $\dot{m}_j$, as the ratio of the specie in the associated tank. This is shown in equations (3.1-3.2).

$$\frac{\dot{m}_j^i}{\dot{m}_j} = \frac{M_l^i}{M_l}, \quad where\ j = l \tag{3.1}$$

$$\dot{m}_j^i = \frac{M_l^i}{M_l} \cdot \dot{m}_j \tag{3.2}$$

The expression for the mass flow of each specie between the mass units, Equation (3.2), is inserted into the expressions of the change of the mass in each of the mass units, equations (3.3-3.5), below.

$$\frac{dM_1^i}{dt} = \dot{m}_{IN}^i - \frac{M_1^i}{M_1}\dot{m}_1 \tag{3.3}$$

$$\frac{dM_2^i}{dt} = \frac{M_1^i}{M_1}\dot{m}_1 - \frac{M_2^i}{M_2}\dot{m}_2 \tag{3.4}$$

$$\frac{dM_3^i}{dt} = \frac{M_2^i}{M_2}\dot{m}_2 - \frac{M_3^i}{M_3}\dot{m}_3 \tag{3.5}$$

For the real model, the mass flow out of the rich MEG pipeline, $\dot{m}_{RM,out}^i$, will be injected into the first mass unit, and therefore replacing $\dot{m}_{IN}$ in Equation (3.3). In the last mass unit the mass flow into the lean MEG pipeline, $\dot{m}_{LM,in}^i$, will be extracted and replacing $\frac{M_3^i}{M_3}\dot{m}_3$ in Equation (3.5).

The mass flow removed from the MEG-recycler, $\dot{m}_{out}^i$, contains both the amount of specie that is removed by the desalination process and the species in the condensate water. This mass flow is modeled to interfere with the first tank, Equation (3.6). The total flow rate between the tanks are modeled to be the same size as the flow out of the last tank, and into the lean MEG pipeline, $\dot{m}_{LM,in}^i$. Therefore the model of each specie i in the MEG-recycler is expressed as shown in equations (3.6-3.9).

$$\frac{dM_1^i}{dt} = \dot{m}_{RM,out}^i - \dot{m}_{OUT}^i - \frac{M_1^i}{M_1}\dot{m}_{LM,in} \tag{3.6}$$

$$\frac{dM_2^i}{dt} = \frac{M_1^i}{M_1}\dot{m}_{LM,in} - \frac{M_2^i}{M_2}\dot{m}_{LM,in} \tag{3.7}$$

$$\vdots$$

$$\frac{dM_{l-1}^i}{dt} = \frac{M_{l-2}^i}{M_{l-2}}\dot{m}_{LM,in} - \frac{M_{l-1}^i}{M_{l-1}}\dot{m}_{LM,in} \tag{3.8}$$

$$\frac{dM_l^i}{dt} = \frac{M_{l-1}^i}{M_{l-1}}\dot{m}_{LM,in} - \dot{m}_{LM,in}^i \tag{3.9}$$

One also needs to model the total mass in each tank. Since the total mass flow between each mass unit is the same for all mass units, and the external input and output mass flows are only interfering with the first mass unit, each of the other mass units, shown in equations (3.11-3.12), is modeled as a mass unit with constant mass, hence the derivatives are zero. The first mass unit is modeled in Equation (3.10). The mass unit is modeled the same way as it is for one specie, as shown in Equation (3.6), but there are some changes in the output mass flows.

For the total mass in the first tank, all the condensate water that is extracted from the rich MEG, $\dot{m}^i_{WAT}$, is removed from the tank. All the salts that is removed from the tank is modeled as only the amount of the three species in the model that is removed, $\frac{\sum_i M^i_1}{M_1}\dot{m}_{DES}$. The MEG/water phase processed through the desalination process are denoted with $\dot{m}_{DES}$. That means the mass flow through the bypass is not represented in the equation, because it do not interfere with the mass in the mass unit. The mass into the first mass unit, $\dot{m}_{IN}$ represent all the inhibitors and the pH-stabilizer injected into the MEG-recycler.

$$\frac{dM_1}{dt} = \dot{m}_{RM,out} + \dot{m}_{IN} - \dot{m}_{WAT} - \dot{m}_{LM,in} - \frac{\sum_i M^i_1}{M_1}\dot{m}_{DES} \tag{3.10}$$

$$\frac{dM_2}{dt} = 0 \tag{3.11}$$

$$\vdots$$

$$\frac{dM_l}{dt} = 0 \tag{3.12}$$

The number of mass units, l, decides the length of the time delay. The level of MEG in the MEG loop will after time drop, since some of the MEG will be removed due to the desalination process. Therefore the tank will be supplied with cleansed MEG on a batch basis. This is not taken account for in this model, to simplify the model.

3.3 Pipelines

In this section the model for both the pipelines, the lean MEG and the rich MEG, are expressed. The mass flows in the pipelines are only modeled for the three species, and not the total mass flow, since the total mass flow is seen upon as the input to the system.

The total mass flow into the lean MEG pipeline is used to model the mass flow of each specie into the lean MEG pipeline. The mass flow into the lean MEG pipeline, $\dot{m}^i_{LM,in}$, is modeled as the mass fraction of the specie in the last MEG-recycle tank, with respect of the total mass of fluid in the tank, times the total

mass flow into the lean MEG pipeline, $\dot{m}_{LM,in}$. This is shown in Equation (3.13). The mass flow for each specie, $\dot{m}^i_{LM,in}$, is denoted with a superscript that shows which specie i it yields for.

The flow rate out of the lean MEG pipeline is modeled as the flow into the pipeline, $\dot{m}^i_{LM,in}$, with a transport delay. τ_1 is the transport delay. This is shown in Equation (3.14).

$$\dot{m}^i_{LM,in} = \frac{M^i_l}{M_l} \cdot \dot{m}_{LM,in} \tag{3.13}$$

$$\dot{m}^i_{LM,out} = e^{-\tau_1 s} \cdot \dot{m}^i_{LM,in} \tag{3.14}$$

In the rich MEG pipeline, the production line, the mass flow for each specie into the pipeline, $\dot{m}^i_{RM,in}$, is the sum of the mass flow out of the lean MEG pipeline, $\dot{m}^i_{LM,out}$, for each specie and the mass flow of formation water, $\dot{m}^i_{FW}$, for each specie. This is shown in Equation (3.15).

The mass flow out of the production line and into the MEG-recycle tank, $\dot{m}^i_{RM,out}$, is modeled as the mass flow into the production line, $\dot{m}^i_{RM,in}$, with a transport delay. τ_2 is the transport delay. This is shown in Equation (3.16) below.

$$\dot{m}^i_{RM,in} = \dot{m}^i_{LM,out} + \dot{m}^i_{FW} \tag{3.15}$$

$$\dot{m}^i_{RM,out} = e^{-\tau_2 s} \cdot \dot{m}^i_{RM,in} \tag{3.16}$$

3.4 Formation water

The model for the formation water for each of the three species is modeled as a constant flow. This because it is uncertain what the process can be expected to produce of each specie. The produced formation water for each specie is also expected to be fairly constant. This is shown in Equation (3.17).

$$\dot{m}^i_{FW} = const \tag{3.17}$$

The total mass flow of formation water is modeled from the amount of three chosen species and the expected concentration these species have in the total formation water flow. This is shown in Equation (3.18).

$$\dot{m}_{FW} = \frac{\alpha_1}{3}\dot{m}^1_{FW} + \frac{\alpha_2}{3}\dot{m}^2_{FW} + \frac{\alpha_3}{3}\dot{m}^3_{FW} \tag{3.18}$$

The variables which contain the expected value for each specie in the formation water mass flow are modeled as dynamical states because of the uncertainty of these parameters. The expected values are difficult to find and they will probably vary with time. Therefore they will be more suited to have as states, where they can adapt to their real value if they are initialized wrong and they can adapt if their real value changes. The model for each of the states are shown in equations (3.19-3.21).

$$\alpha_1 = const \tag{3.19}$$
$$\alpha_2 = const \tag{3.20}$$
$$\alpha_3 = const \tag{3.21}$$

3.5 Desalination and water extraction

The mass flow through the desalination process is divided into the bypass, which is the first pipeline into the mixer, and the pipeline which is desalinated. The mass flow through the desalination will be cleansed for all salts that are contained in the mass flow. For the modeling of the desalination the bypass pipeline is ignored, because it does not make any change for the mass unit or the amount of species in the mass unit.

The species removed from the first mass unit is dependent on two mass flows. That is the species removed by the desalination plant and the species contained with the condensate water extraction from the MEG-recycler. For both mass flows, all the species that are contained in them are modeled to be removed. Therefore the species removed from the MEG-recycler depends on the fraction of specie in the first mass unit and the two mass flows. This is shown in Equation (3.22).

$$\dot{m}^i_{OUT} = \frac{M^i_1}{M_1} \cdot (\dot{m}_{WAT} + \dot{m}_{DES}) \tag{3.22}$$

The amount of removed species from the MEG-regenerator can also be removed as a constant that is allowed to change value. This is shown in Equation (3.23).

$$\dot{m}^i_{OUT} = const \tag{3.23}$$

The alternative expression for the mass flow removed from the MEG-regenerator, Equation (3.23), is made because there is some uncertainty in the expression above, Equation (3.22).

Chapter 4

Numerical solver and model discretization

First in this chapter the numerical solvers used to solve the differential equations of the model is described. In the next part the discretization of the model is done with use of the numerical solver. In the last part the linear test function is applied to test if the system, including the numerical solver, is stable.

4.1 Numerical solver for differential equations

The numerical solver used to solve the differential equations is the Euler method. The method will be described in this section.

4.1.1 Euler method

The numerical solver used for the discretization of the model is chosen to be the Euler method. This is done because the Euler method is easy to implement and will not complicate the model any further. The Euler method is an explicit Runge-Kutta method of order 1. In Equation (4.2) the Euler method is displayed, the system is on the form as shown in Equation (4.1).

For each step the explicit Euler method makes an error, that is denoted with $O(h^2)$. The error is caused by the rounding of the Taylor series that is used to develop the numerical solver. More can be found of this in [4].

$$\dot{\boldsymbol{y}} = \boldsymbol{f}(\boldsymbol{y}_n) \tag{4.1}$$

$$\boldsymbol{y}_{n+1} = \boldsymbol{y}_n + \Delta t \cdot \boldsymbol{f}(\boldsymbol{y}_n) + O(h^2) \tag{4.2}$$

The time step is represented with the letter Δt.

4.2 Model discretization

The discretization of the model is based upon the model derived in Chapter 3, Model development. The method used to handle derivatives is the Euler method. The stability of the numerical solver is examined in the next section. As in the previous chapter, the discretization is just shown for one specie.

4.2.1 The MEG-regeneration tank

Since the explicit Euler method is used to solve the differential equations, the amount of each specie in the mass units is the value it had at the former time steps in addition to the input and output mass flows. This yield for each specie, and the output and input mass flows has to be multiplied with the size of the time step.

As described in the previous chapter, the external input and output streams are set to interfere with the first tank, this is shown in Equation (4.3). The values the input and output mass flow is using to find the mass of the mass unit is also from the former time step, (t_{k-1}).

$$\begin{aligned} M_1^i(t_k) = M_1^i(t_{k-1}) + \Delta t[&\dot{m}_{RM,m}^i(t_{k-1}) - \dot{m}_{OUT}^i(t_{k-1}) - \\ &\frac{M_1^i(t_{k-1})}{M_1(t_{k-1})} \cdot \dot{m}_{LM,1}(t_{k-1})] \end{aligned} \tag{4.3}$$

$$\begin{aligned} M_2^i(t_k) = M_2^i(t_{k-1}) + \Delta t[&\frac{M_1^i(t_{k-1})}{M_1(t_{k-1})} \cdot \dot{m}_{LM,1}(t_{k-1}) - \\ &\frac{M_2^i(t_{k-1})}{M_2(t_{k-1})} \cdot \dot{m}_{LM,1}(t_{k-1})] \end{aligned} \tag{4.4}$$

$$\vdots$$

$$\begin{aligned} M_{l-1}^i(t_k) = M_{l-1}^i(t_{k-1}) + \Delta t[&\frac{M_{l-2}^i(t_{k-1})}{M_{l-2}(t_{k-1})} \cdot \dot{m}_{LM,1}(t_{k-1}) - \\ &\frac{M_{l-1}^i(t_{k-1})}{M_{l-1}(t_{k-1})} \cdot \dot{m}_{LM,1}(t_{k-1})] \end{aligned} \tag{4.5}$$

$$M_l^i(t_k) = M_l^i(t_{k-1}) + \Delta t[\frac{M_{l-1}^i(t_{k-1})}{M_{l-1}(t_{k-1})} \cdot \dot{m}_{LM,1}(t_{k-1}) - \dot{m}_{LM,1}^i(t_{k-1})] \tag{4.6}$$

The total mass in each tank is also discretized. Since all inputs and outputs is modeled to interfere with the first tank, the first tank is modeled in the same way as is in Equation (4.3) with one specie, but now with the total mass rates. This is shown in Equation (4.7). The mass flows of the input and outputs used to find the new mass of the mass unit is from the former time step, (t_{k-1}).

Since the mass in the remaining mass units is modeled to be constant, the mass is set to the mass it had at the last time step, shown in equations (4.8-4.9).

$$M_1(t_k) = M_1(t_{k-1}) + \Delta t[\dot{m}_{RM,m}(t_{k-1}) + \dot{m}_{IN}(t_{k-1}) - \dot{m}_{WAT}(t_{k-1}) - \frac{\sum M_1^i(t_{k-1})}{M_1(t_{k-1})} \cdot \dot{m}_{DES} - \dot{m}_{LM,1}(t_{k-1})] \tag{4.7}$$

$$M_2(t_k) = M_2(t_{k-1}) \tag{4.8}$$

$$\vdots$$

$$M_l(t_k) = M_l(t_{k-1}) \tag{4.9}$$

4.2.2 The pipelines

The first state in the lean MEG pipeline, the injection line, is on the same form as in Chapter 3, Model development, Equation (3.13). The difference is that the flow rate of one specie into the pipeline, $\dot{m}^i_{LM,1}(t_k)$, is calculated from states one time step behind. This is shown in Equation (4.10).

The rest of the states in the lean MEG pipeline is modeled as the former state from last time step, shown in equations (4.11-4.12). This is done to get the effect of a transport delay and these states represents the transport delay in Equation (3.14). Each state is set to be the value the previous state had at the former time step, therefore the mass in the pipeline will stay unchanged throughout the pipeline. There will be no changes in composition in the pipelines, and the velocity through the pipeline will always be the same.

The length of the transport delay can be changed by adjusting the number of states in the lean MEG pipeline. The length will then be the number of states, represented with k, times the size of the time step.

$$\dot{m}^i_{LM,1}(t_k) = \frac{M_l^i(t_{k-1})}{M_l(t_{k-1})} \cdot \dot{m}_{LM,1}(t_{k-1}) \tag{4.10}$$

$$\dot{m}^i_{LM,2}(t_k) = \dot{m}^i_{LM,1}(t_{k-1}) \tag{4.11}$$

$$\vdots$$

$$\dot{m}^i_{LM,k}(t_k) = \dot{m}^i_{LM,k-1}(t_{k-1}) \tag{4.12}$$

In the rich MEG pipeline, the production line, the first state is the sum of the final state in the lean MEG pipeline, $\dot{m}^i_{LM,k}$, for each specie and the mass flow for each specie of the formation water, $\dot{m}^i_{FW}$. This is shown in Equation (4.13).

The rest of the states are modeled as the former state from last time step, shown in equations (4.14-4.15) below. This is, like the lean MEG pipeline, done to

represent the transport delay in the model, Equation (3.16). As for the lean MEG pipeline, the transport delay in the production line is determined by the number of states in the pipeline, m, times the size of the time step.

$$\dot{m}^i_{RM,1}(t_k) = \dot{m}^i_{LM,k}(t_{k-1}) + \dot{m}^i_{FW}(t_{k-1}) \tag{4.13}$$
$$\dot{m}^i_{RM,2}(t_k) = \dot{m}^i_{RM,1}(t_{k-1}) \tag{4.14}$$
$$\vdots$$
$$\dot{m}^i_{RM,m}(t_k) = \dot{m}^i_{RM,m-1}(t_{k-1}) \tag{4.15}$$

4.2.3 The formation water

The model for the formation water for each specie is modeled as a constant flow, which means the flow is seen upon as unchanged from last time step. This is shown in Equation (4.16).

$$\dot{m}^i_{FW}(t_k) = \dot{m}^i_{FW}(t_{k-1}) \tag{4.16}$$

The total flow rate of formation water is modeled from the amount of the three chosen species and the expected concentration these specie have in the total formation water flow. This is shown in Equation (4.17).

$$\begin{aligned}\dot{m}_{FW}(t_k) =& \frac{\alpha_1(t_{k-1})}{3}\dot{m}^1_{FW}(t_{k-1}) + \frac{\alpha_2(t_{k-1})}{3}\dot{m}^2_{FW}(t_{k-1}) \\ &+ \frac{\alpha_3(t_{k-1})}{3}\dot{m}^3_{FW}(t_{k-1})\end{aligned} \tag{4.17}$$

The states used to predict the amount of total formation water from the species in the formation water is discretized as shown in equations (4.18-4.20). They are all set to their value from the last time step.

$$\alpha_1(t_k) = \alpha_1(t_k - 1) \tag{4.18}$$
$$\alpha_2(t_k) = \alpha_2(t_k - 1) \tag{4.19}$$
$$\alpha_3(t_k) = \alpha_3(t_k - 1) \tag{4.20}$$

4.2.4 Desalination and water extraction

The removed species from the MEG-recycler is at the same form as shown is previous chapter, Chapter 3. The mass stream out for each specie, $\dot{m}^i_{OUT}(t_k)$, is the same ratio of the total mass flow out as the ratio between the specie and the total amount of mass in the tank.

$$\dot{m}^i_{OUT}(t_k) = \frac{M^i_1}{M_1}(t_k - 1) \cdot (\dot{m}_{WAT}(t_{k-1}) + \dot{m}_{DES}(t_{k-1})) \tag{4.21}$$

The alternative method to model the removed mass from the first mass unit from Equation (3.23), is discretized to be the same mass flow it had at the former time step, since it was modeled as a constant. This is shown in Equation (4.22).

$$\dot{m}^i_{OUT}(t_k) = \dot{m}^i_{OUT}(t_{k-1}) \tag{4.22}$$

4.3 Linear test function

The linear test function is a tool applied on the system, consisting of the model and the numerical solver, to find out if the numerical integrator will be stable. The linear test function is on the form shown in Equation (4.23) below. The theory in this chapter is taken from [4].

$$\dot{\boldsymbol{x}} = \boldsymbol{\lambda x} \tag{4.23}$$

The system is on the form shown in Equation (4.24) and the linear test function is ensured if Equation (4.25) is fulfilled.

$$\boldsymbol{x_{n+1}} = \boldsymbol{R}(h\boldsymbol{\lambda}) \cdot \boldsymbol{x_n} \tag{4.24}$$

$$|\boldsymbol{R}(h\boldsymbol{\lambda})| \leq \mathbf{1} \tag{4.25}$$

$$|\boldsymbol{x_{n+1}}| \leq |\boldsymbol{x_n}| \tag{4.26}$$

When the linear test function is ensured it means that the system not violates Equation (4.26). That will ensure that each step will reduce the absolute value of the states, $\boldsymbol{x_n}$.

4.3.1 Linear test function on the Euler method

The linear test function is performed on the system with the Euler method. The elements in the stability function, $\boldsymbol{R}(h\boldsymbol{\lambda})$, is shown in equations (4.27-4.31) beneath.

The elements in the stability function are the states in the system where the Euler method has been taken in use. That means that all the states for the mass for each specie in all the tanks, equations (4.3-4.6), are included. The total mass in the first tank is also included, Equation (4.7). In total the stability function will consist of l times three, plus one, elements. As can be seen in equations (4.27-4.29) the elements are the same for each specie, since the equations are only dependent on the total input lean MEG mass flow and the total mass in each tank.

$$R_1^i = 1 - \frac{\dot{m}_{LM,1}}{M_1} \cdot h, \quad \forall i \tag{4.27}$$

$$R_2^i = 1 - \frac{\dot{m}_{LM,1}}{M_2} \cdot h, \quad \forall i \tag{4.28}$$

$$\vdots$$

$$R_{l-1}^i = 1 - \frac{\dot{m}_{LM,1}}{M_{l-1}} \cdot h, \quad \forall i \tag{4.29}$$

$$R_l^i = 1 - \dot{m}_{LM,1}^i \cdot h, \quad \forall i \tag{4.30}$$

$$R_{l+1} = 1 \tag{4.31}$$

Since the stability function have to fulfill the Equation (4.25) above, the variables have to fulfill the equations beneath, (4.32-4.35). In these equations only the unique conditions are listed.

There are $l+2$ conditions that needs to be fulfilled. The condition from Equation (4.31) is not included since it always will be fulfilled and the $3 * l$ conditions from equations (4.27-4.29) are reduced to $l - 1$ conditions because they are the same for each specie. The Equation (4.35) represents the three conditions for the three species.

$$0 < \frac{\dot{m}_{LM,1}}{M_1} < \frac{2}{h} \tag{4.32}$$

$$0 < \frac{\dot{m}_{LM,1}}{M_2} < \frac{2}{h} \tag{4.33}$$

$$\vdots$$

$$0 < \frac{\dot{m}_{LM,1}}{M_{l-1}} < \frac{2}{h} \tag{4.34}$$

$$0 < \dot{m}_{LM,1}^i < \frac{2}{h}, \quad \forall i \tag{4.35}$$

It is assumed that all the variables, $\dot{m}_{LM,1}$, M_1, M_2, M_3 and $\dot{m}^i_{LM,1}$, is all nonnegative. This is mostly the case, but the three inputs to the lean MEG pipeline, $\dot{m}^i_{LM,1}$, for each specie is near zero, and these states can therefore be in danger to become negative. If they are assumed to be nonnegative one can see that the fraction between the input lean MEG mass rate and the mass in the $l-1$ first tanks has to be less than two divided on the step length. The step length is for this system most practically one, so the fraction has to be smaller than two.

4.3.2 Change of numerical solver

From the analysis done in the linear test function we have these eigenvalues, $\boldsymbol{\lambda}$, that are shown in equations (4.36-4.40). For equations (4.36-4.38) there is one equation for each specie, but it is the same for all three species, so they are only listed as one.

$$\lambda_1 = \frac{\dot{m}_{LM,1}}{M_1} \tag{4.36}$$

$$\lambda_2 = \frac{\dot{m}_{LM,1}}{M_2} \tag{4.37}$$

$$\vdots$$

$$\lambda_{l-1} = \frac{\dot{m}_{LM,1}}{M_{l-1}} \tag{4.38}$$

$$\lambda_l = \dot{m}^i_{LM,1}, \quad \forall i \tag{4.39}$$

$$\lambda_{l+1} = 0 \tag{4.40}$$

The masses in the mass unit are unchanged for all the mass units except the first mass unit, and the initial value for each tank can be set arbitrarily, therefore it is no problem to control the corresponding eigenvalues. That will also yield on the first eigenvalue since the mass in the first tank will ideally stay at the same amount. The mass rate of the different species into the lean MEG pipeline will be fairly small amounts, and should therefore also be constrained by a small bound.

Table 4.1: Expected eigenvalues for the model.

λ	Minimum eigenvalue	Maximum eigenvalue
λ_1	0	1
λ_2	0	1
λ_{l-1}	0	1
λ_l	0	0.01
λ_{l+1}	0	0

Since all the expected values of the eigenvalues listed in Table 4.1 fulfills the conditions of the Euler method there is no need to change the numerical solver. The constraints for the Euler method are that the expected eigenvalues are between zero and two.

Chapter 5

Kalman filter

For this system an unscented Kalman filter is chosen at the expense of a regular Kalman filter or an extended Kalman filter. With an extended Kalman filter (or regular Kalman filter) one need to linearize the model around some initial points to be able to propagate the mean and the covariance for the state. This means the system has to be re-linearized if the system moves away from the initial points. It makes the extended Kalman filter (or regular Kalman filter) more difficult to tune and can give unreliable estimates when there are severe nonlinearities [14]. With the unscented Kalman filter, the model does not need to be linearized and the system will be more robust if it drifts away from its initial states.

In this chapter the standard Kalman filter will be explained before the unscented Kalman filter is explained. Both Kalman filters are explained at discrete time.

5.1 The discrete Kalman filter

The theory in this part is taken form [2]. The discrete Kalman filter can be applied on a system on the form displayed in equations (5.1-5.2) below. $\boldsymbol{x_k}$ is the process state vector at time t_k, $\boldsymbol{\Phi_k}$ is the relation between $\boldsymbol{x_k}$ and $\boldsymbol{x_{k+1}}$ and $\boldsymbol{w_k}$ is the process noise matrix. The state vector consists of both the measured states and the parameters of the system. $\boldsymbol{y_k}$ is the measurement vector at time t_k, $\boldsymbol{H_k}$ is the relation between the states and the measurements, and $\boldsymbol{v_k}$ is the observation noise. $\boldsymbol{\Phi_k}$ and $\boldsymbol{H_k}$ can be time invariant and will then be denoted as the constants $\boldsymbol{\Phi}$ and constant $\boldsymbol{H}$.

$$\boldsymbol{x_{k+1}} = \boldsymbol{\Phi_k x_k} + \boldsymbol{w_k} \tag{5.1}$$

$$\boldsymbol{y_k} = \boldsymbol{H_k x_k} + \boldsymbol{v_k} \tag{5.2}$$

The covariance matrices for the process error and the observation error are given in equations (5.3-5.4). $E[x]$ symbols the expected value of x.

$$E[\boldsymbol{w_k}\boldsymbol{w_i^T}] = \boldsymbol{Q_k}, \quad i = k \tag{5.3}$$
$$E[\boldsymbol{v_k}\boldsymbol{v_i^T}] = \boldsymbol{R_k}, \quad i = k \tag{5.4}$$

All other combinations of the covariance matrices gives the expected value of zero. The same yields for all combinations between the process error and the observation error. From equations (5.3-5.4) it can be seen that $\boldsymbol{Q_k}$ expresses the expected error in the system state update $\boldsymbol{\Phi_k}$, and that $\boldsymbol{R_k}$ expresses the expected value of the error in the measurements, $\boldsymbol{H_k}$.

The Kalman filter has to be initialized before the simulation of the system can start. The *a priori* estimate of the state vector and the corresponding error covariance matrix is initialized as shown in equations (5.5-5.6) below. The error covariance matrix is usually initialized as a diagonal matrix, with values only on the diagonal.

$$\hat{\boldsymbol{x}}_{\boldsymbol{0}}^{-} = E(\boldsymbol{x_0}) \tag{5.5}$$
$$\boldsymbol{P_0^-} = E[(\boldsymbol{x_0} - \hat{\boldsymbol{x}}_{\boldsymbol{0}}^{-})(\boldsymbol{x_0} - \hat{\boldsymbol{x}}_{\boldsymbol{0}}^{-})^T] \tag{5.6}$$

The "hat" denotes that it is an estimate and the "super minus" denotes that the estimate has not yet been adjusted with respect of the measurements. When a vector or a matrix only has an "hat" and not a "super minus" it is the *a posteriori* estimate. It means the measurements is taken into account, and for the state vector this is called the assimilated state vector. $\boldsymbol{P_k}$ describes the error covariance between the real states of the system and the *a priori* estimated states.

5.1.1 The Kalman filter loop

The Kalman filter can be seen upon as a loop that repeats itself for each time step. In Figure 5.1 the loop of the Kalman filter for each iteration is displayed.

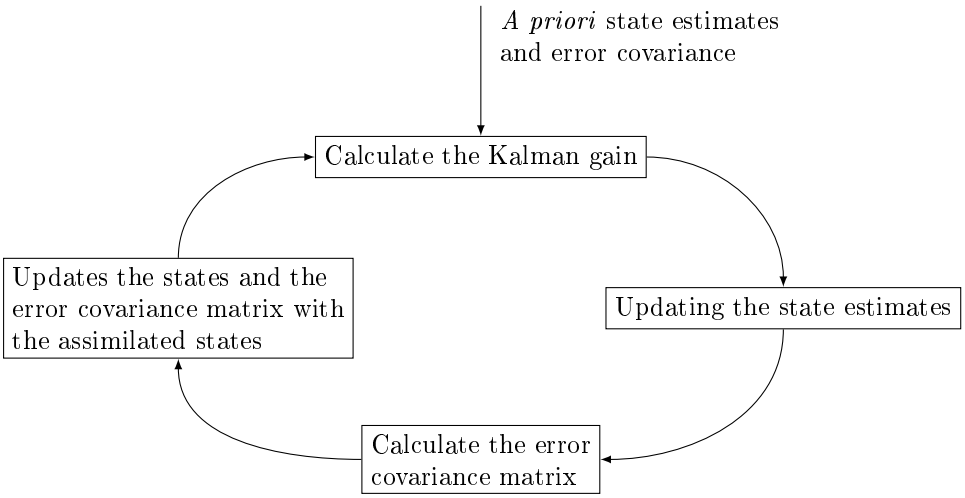

Figure 5.1: The Kalman filter loop, inspired by the figure on page 219 in [2]. The loop is repeated for each iteration.

When the Kalman filter is initialized the filtering can begin. The first step in the Kalman filter loop is to update the Kalman gain, $\boldsymbol{K_k}$, as shown in Equation (5.7).

$$\boldsymbol{K_k} = \boldsymbol{P_k^-}\boldsymbol{H_k^T}(\boldsymbol{H_k}\boldsymbol{P_k^-}\boldsymbol{H_k^T} + \boldsymbol{R_k})^{-1} \tag{5.7}$$

$\boldsymbol{K_k}$ represents the Kalman gain which describes the ratio between the certainty of the measurements and the predicted measurements, given by the state estimate. $\boldsymbol{K_k}$ is set to minimize the estimation error.

When the Kalman gain is computed the estimates can be updated with respect of the measurements. It makes the *a priori* estimate to become an *a posteriori* estimate. This is done as displayed in Equation (5.8).

$$\hat{\boldsymbol{x}}_{\boldsymbol{k}} = \hat{\boldsymbol{x}}_{\boldsymbol{k}}^- + \boldsymbol{K_k}(\boldsymbol{y_k} - \boldsymbol{H_k}\hat{\boldsymbol{x}}_{\boldsymbol{h}}^-) \tag{5.8}$$

The calculated $\hat{\boldsymbol{x}}_{\boldsymbol{k}}$ is the assimilated state estimate.

Further the *a posteriori* error covariance for the updated estimates can be calculated as shown in Equation (5.10) below.

$$\boldsymbol{P_k} = (\boldsymbol{I} - \boldsymbol{K_k}\boldsymbol{H_k})\boldsymbol{P_k^-} \tag{5.9}$$

When the *a posteriori* estimates of the state vector and the error covariance matrix is calculated, the last step of the Kalman filter loop can be conducted. This step updates the states and the error covariance in respect to the model.

$$\hat{\boldsymbol{x}}_{\boldsymbol{k+1}}^{-} = \boldsymbol{\Phi}\hat{\boldsymbol{x}}_{\boldsymbol{k}} \tag{5.10}$$

$$\boldsymbol{P}_{\boldsymbol{k+1}}^{-} = \boldsymbol{\Phi}\boldsymbol{P}_{\boldsymbol{k}}\boldsymbol{\Phi}_{\boldsymbol{k}}^{\boldsymbol{T}} + \boldsymbol{Q}_{\boldsymbol{k}} \tag{5.11}$$

Then the time step is changed from t_k to t_{k+1} and the Kalman filter loop will again be executed.

5.2 The discrete unscented Kalman filter

The unscented Kalman filter is explained with a discrete model. The theory in this section is taken from [14]. An unscented Kalman filter is based upon an unscented transformation. The problem with a linearization of a nonlinear system is that the linearization only yields for one specific point of the system. The main principle of the unscented transformation is to perform a nonlinear transformation for several points of the state space. These points are called sigma points.

One start with the n-state nonlinear system on the form given in equations (5.12-5.13). $\boldsymbol{w_k}$ and $\boldsymbol{v_k}$ is the process noise and measurement noise, respectively. As opposed to the model used in the regular Kalman filter, displayed in equations (5.1-5.2), the model used in an unscented Kalman filter can be a nonlinear model.

$$\boldsymbol{x_{k+1}} = \boldsymbol{f}(\boldsymbol{x_k}, \boldsymbol{u_k}, t_k) + \boldsymbol{w_k} \tag{5.12}$$

$$\boldsymbol{y_k} = \boldsymbol{h}(\boldsymbol{x_k}, t_k) + \boldsymbol{v_k} \tag{5.13}$$

As for the Kalman filter, $\boldsymbol{Q_k}$ and $\boldsymbol{R_k}$ represents the expected error in the systems state updates and the measurements, respectively.

The initialization of the unscented Kalman filter is done in the same form as the regular Kalman filter, and is initialized as shown below in equations (5.14-5.15). As for the regular Kalman filter, the error covariance matrix is usually initialized as diagonal matrix, with values only on the diagonal.

$$\hat{\boldsymbol{x}}_{\boldsymbol{0}}^{+} = E(\boldsymbol{x_0}) \tag{5.14}$$

$$\boldsymbol{P}_{\boldsymbol{0}}^{+} = E[(\boldsymbol{x_0} - \hat{\boldsymbol{x}}_{\boldsymbol{0}}^{+})(\boldsymbol{x_0} - \hat{\boldsymbol{x}}_{\boldsymbol{0}}^{+})^T] \tag{5.15}$$

5.2.1 State update equations

The sigma points are used so the states can propagate from time step t_{k-1} to t_k. There are made $2n$ sigma points, $\tilde{\boldsymbol{x}}^{(\boldsymbol{i})}$. This is shown in equations (5.16-5.18).

$$\hat{\boldsymbol{x}}_{\boldsymbol{k-1}}^{(\boldsymbol{i})} = \hat{\boldsymbol{x}}_{\boldsymbol{k-1}}^{+} + \tilde{\boldsymbol{x}}^{(\boldsymbol{i})} \quad i = 1, ..., 2n \tag{5.16}$$

$$\tilde{\boldsymbol{x}}^{(\boldsymbol{i})} = (\sqrt{n\boldsymbol{P}_{\boldsymbol{k-1}}^{+}})_i^T \quad i = 1, ..., n \tag{5.17}$$

$$\tilde{\boldsymbol{x}}^{(\boldsymbol{n+i})} = -(\sqrt{n\boldsymbol{P}_{\boldsymbol{k-1}}^{+}})_i^T \quad i = 1, ..., n \tag{5.18}$$

$(\sqrt{n\boldsymbol{P}_{\boldsymbol{k-1}}^{+}})_i^T$ represent the ith row of $(\sqrt{n\boldsymbol{P}_{\boldsymbol{k-1}}^{+}})^T$. The size of the model, represented with the number of states, n, is used to decide the spread of the sigma points. This is done because a bigger model is likely to be more uncertain, and therefore each state needs a bigger initial "area" when estimating.

Cholesky factorization

The Cholesky factorization can be used to find the square root of the error covariance matrix times the number of state, $(\sqrt{n\boldsymbol{P}_{\boldsymbol{k-1}}^{+}})$. The Cholesky factorization on a matrix $\boldsymbol{P}$ produces a matrix $\boldsymbol{C}$. this is shown in Equation (5.19).

$$\boldsymbol{C}\boldsymbol{C}^{\boldsymbol{T}} = \boldsymbol{P} \tag{5.19}$$

The matrix $\boldsymbol{P}$ has to be positive definite for the Cholesky factorization to be able to succeed [9].

Further the system equations are used to calculate the new states based on the sigma points. The system equations is the same as derived in Equation (5.12) and propagates a vector of sigma points for each state estimate shown in Equation (5.20).

$$\hat{\boldsymbol{x}}_{\boldsymbol{k}}^{(\boldsymbol{i})} = \boldsymbol{f}(\hat{\boldsymbol{x}}_{\boldsymbol{k-1}}^{(\boldsymbol{i})}, \boldsymbol{u_k}, t_k) \tag{5.20}$$

Constraints on the state estimates can be introduced by applying an algorithm on these equations. This will be described in Section 5.3 below.

To find an *a priori* state estimate the mean value for all the sigma points are taken. This is displayed in Equation (5.21).

$$\hat{\boldsymbol{x}}_{\boldsymbol{k}}^{-} = \frac{1}{2n}\sum_{i=1}^{2n}\hat{\boldsymbol{x}}_{\boldsymbol{k}}^{(\boldsymbol{i})} \tag{5.21}$$

The same approach is used when the *a priori* error covariance is estimated, which is shown in Equation (5.22).

$$\boldsymbol{P}_{\boldsymbol{k}}^{-} = \frac{1}{2n}\sum_{i=1}^{2n}(\hat{\boldsymbol{x}}_{\boldsymbol{k}}^{(\boldsymbol{i})} - \hat{\boldsymbol{x}}_{\boldsymbol{k}}^{-})(\hat{\boldsymbol{x}}_{\boldsymbol{k}}^{(\boldsymbol{i})} - \hat{\boldsymbol{x}}_{\boldsymbol{k}}^{-})^T + \boldsymbol{Q}_{\boldsymbol{k-1}} \tag{5.22}$$

5.2.2 Measurement update equations

First the new sigma points, $\boldsymbol{x}_{\boldsymbol{k}}^{(\boldsymbol{i})}$, is calculated with the new *a priori* state estimates and error covariance from the state update equations. The sigma points are calculated the same way as equations (5.16-5.18) above. And is displayed below in equations (5.23-5.25).

$$\hat{\boldsymbol{x}}_{\boldsymbol{k}}^{(\boldsymbol{i})} = \hat{\boldsymbol{x}}_{\boldsymbol{k}}^{-} + \tilde{\boldsymbol{x}}^{(\boldsymbol{i})} \quad i = 1, ..., 2n \tag{5.23}$$

$$\tilde{\boldsymbol{x}}^{(\boldsymbol{i})} = (\sqrt{n\boldsymbol{P}_{\boldsymbol{k}}^{-}})_i^T \quad i = 1, ..., n \tag{5.24}$$

$$\tilde{\boldsymbol{x}}^{(\boldsymbol{n+i})} = -(\sqrt{n\boldsymbol{P}_{\boldsymbol{k}}^{-}})_i^T \quad i = 1, ..., n \tag{5.25}$$

Then the measurement equations, $\boldsymbol{h}(\hat{\boldsymbol{x}}_{\boldsymbol{k}}^{(\boldsymbol{i})}, t_k)$, are used to propagate the measurements, $\hat{\boldsymbol{y}}_{\boldsymbol{k}}$, from the sigma points as showed in Equation (5.26).

$$\hat{\boldsymbol{y}}_{\boldsymbol{k}}^{(\boldsymbol{i})} = \boldsymbol{h}(\hat{\boldsymbol{x}}_{\boldsymbol{k}}^{(\boldsymbol{i})}, t_k) \tag{5.26}$$

Further the mean of the all the sigma points is taken to find a mean value of the measurement vector. This is displayed in Equation (5.27).

$$\hat{\boldsymbol{y}}_{\boldsymbol{k}} = \frac{1}{2n}\sum_{i=1}^{2n}\hat{\boldsymbol{y}}_{\boldsymbol{k}}^{(\boldsymbol{i})} \tag{5.27}$$

In Equation (5.28), the error covariance matrix for the predicted measurements is calculated by using the sigma point for the measurements and the mean measurements.

$$\boldsymbol{P_y} = \frac{1}{2n}\sum_{i=1}^{2n}(\hat{\boldsymbol{y}}_{\boldsymbol{k}}^{(\boldsymbol{i})} - \hat{\boldsymbol{y}}_{\boldsymbol{k}})(\hat{\boldsymbol{y}}_{\boldsymbol{k}}^{(\boldsymbol{i})} - \hat{\boldsymbol{y}}_{\boldsymbol{k}})^T + \boldsymbol{R_k} \tag{5.28}$$

The cross covariance between the states and the measurements is found as shown below, Equation (5.29).

$$\boldsymbol{P_{xy}} = \frac{1}{2n}\sum_{i=1}^{2n}(\hat{\boldsymbol{x}}_{\boldsymbol{k}}^{(\boldsymbol{i})} - \hat{\boldsymbol{x}}_{\boldsymbol{k}}^{-})(\hat{\boldsymbol{y}}_{\boldsymbol{k}}^{(\boldsymbol{i})} - \hat{\boldsymbol{y}}_{\boldsymbol{k}})^T \tag{5.29}$$

Then the results found in the state update and measurements update equations can be used to calculate the Kalman gain, the *a posteriori* state vector and the *a posteriori* error covariance matrix for the states. The calculations is displayed in equations (5.30-5.32).

$$\boldsymbol{K_k} = \boldsymbol{P_{xy}}\boldsymbol{P_y^-} \tag{5.30}$$

$$\hat{\boldsymbol{x}}_{\boldsymbol{k}}^{+} = \hat{\boldsymbol{x}}_{\boldsymbol{k}}^{-} + \boldsymbol{K_k}(\boldsymbol{y_k} - \hat{\boldsymbol{y}}_{\boldsymbol{k}}) \tag{5.31}$$

$$\boldsymbol{P_k^+} = \boldsymbol{P_k^-} - \boldsymbol{K_k}\boldsymbol{P_y}\boldsymbol{K_k^T} \tag{5.32}$$

When this is done the whole procedure must be done again to the simulation is finished.

5.3 Constraints on the states

In [13] R. Kandepu, L. Imsland and B. A. Foss develops an algorithm which makes it possible to introduce constraints for the state estimates in the unscented Kalman filter. The method projects the states that violate the constraints into the boundary of the feasible region. The method is in [13] shown to increase the accuracy of the estimates in compared to an unscented Kalman filter without the algorithm implemented.

The algorithm start with the $2n$ sigma points calculated in Equation (5.16). For each of the sigma points that lays outside the feasible region the sigma point is projected into the boundary of the feasible region. This is shown in Equation (5.33). $P(x)$ means the projection of x.

$$\hat{\boldsymbol{x}}_{\boldsymbol{k-1}}^{(\boldsymbol{i}),\boldsymbol{C}} = P(\hat{\boldsymbol{x}}_{\boldsymbol{k-1}}^{(\boldsymbol{i})}) \tag{5.33}$$

The new sigma points, which includes the projected sigma points, are denoted with $\hat{\boldsymbol{x}}_{\boldsymbol{k-1}}^{\boldsymbol{(i),C}}$.

Then the state update is done with the state model, it is displayed in Equation (5.34) below. Instead of the old sigma points, $\hat{\boldsymbol{x}}_{\boldsymbol{k-1}}^{\boldsymbol{(i)}}$, the new projected sigma points, $\hat{\boldsymbol{x}}_{\boldsymbol{k-1}}^{\boldsymbol{(i),C}}$, is used to calculate the propagation of the state vector.

$$\hat{\boldsymbol{x}}_{\boldsymbol{k}}^{\boldsymbol{(i)}} = \boldsymbol{f}(\hat{\boldsymbol{x}}_{\boldsymbol{k-1}}^{\boldsymbol{(i),C}}, \boldsymbol{u_k}, t_k) \tag{5.34}$$

After the propagation of the state vector is conducted, those propagated sigma points that now lays outside the constraints are projected into the boundary of the feasible region. This projection is shown in Equation (5.35).

$$\hat{\boldsymbol{x}}_{\boldsymbol{k}}^{\boldsymbol{(i),C}} = P(\hat{\boldsymbol{x}}_{\boldsymbol{k}}^{\boldsymbol{(i)}}) \tag{5.35}$$

After this is done the unscented Kalman filter can be proceeded as normal.

Chapter 6

System implementation

In this chapter the implementation of the system will be described. First the environments used to implement the system and the preprocessing of the data is explained. In the other part the implementation related to the unscented Kalman filter described in Chapter 5 and the discrete model from Chapter 4, is described.

6.1 Environments and preprocessing of data

The model with the associated Kalman filter, is implemented in Matlab. Matlab is a high-level language, and environment, made by Mathworks. It is a good tool for numerical calculations, programming, plotting and simulations among others [7]. In Matlab the system can be simulated with both real production data from the Snøhvit field and test data produced in Matlab.

The real data from the process is collected from Statoils system Aspen Process Explorer (APE), developed by AspenTech. In Aspen Process Explorer one can pick out the required data, the period of interest and choose the data sample frequency. If the data sample frequency for retrieving data do not match with the measurement frequency, Aspen Process Explorer has several functions to adjust the data. One of them is to average the process data.

The real production data obtained from Aspen Process Explorer is displayed in Table 6.1 below. The table shows which unit the data has in Aspen Process Explorer and which of the units that are converted or scaled in Matlab.

Table 6.1: The data imported from Aspen Process Explorer. The data name and variable name is the same as used in Matlab.

Data	Variable	Unit in APE	Unit in MATLAB
Rich MEG total mass flow	$\dot{m}_{RM}$	ton/h	kg/h
Lean MEG total mas flow	$\dot{m}_{LM}$	ton/h	kg/h
pH-stabilizer	$\dot{m}_{IN}$	kg/h	kg/h
Scale inhibitor	$\dot{m}_{IN}$	kg/h	kg/h
Removed water	$\dot{m}_{WAT}$	kg/h	kg/h
Rate of Mg^{2+} in rich MEG	$\dot{m}_{RM,Mg^{2+}}$	mg/l	kg/h
Rate of Mg^{2+} in lean MEG	$\dot{m}_{LM,Mg^{2+}}$	mg/l	kg/h
Rate of Ca^{2+} in rich MEG	$\dot{m}_{RM,Ca^{2+}}$	mg/l	kg/h
Rate of Ca^{2+} in lean MEG	$\dot{m}_{LM,Ca^{2+}}$	mg/l	kg/h
Rate of Sr^{2+} in rich MEG	$\dot{m}_{RM,Sr^{2+}}$	mg/l	kg/h
Rate of Sr^{2+} in lean MEG	$\dot{m}_{LM,Sr^{2+}}$	mg/l	kg/h
Upstream desalination	$\dot{m}_{UP}$	kg/h	
Downstream desalination	$\dot{m}_{DWN}$	kg/h	
Bypass desalination	$\dot{m}_{BY}$	kg/h	
wt% MEG in rich MEG	$\text{wt\%}_{RM}$	%	
wt% MEG in lean MEG	$\text{wt\%}_{LM}$	%	
Density in rich MEG	ρ_{RM}	g/cm^3	
Density in lean MEG	ρ_{LM}	g/cm^3	

The data in the first block is found both in Aspen Process Explorer and Matlab and the only change is in some cases the scaling of the unit. The second block consists of concentrations that needs data from the last block to be represented with the right unit in Matlab. The last block is measurements from Aspen Process Explorer that is not used directly, but used to make other variables in Matlab.

All the flow rates are scaled to be at the form $[kg/h]$, while all densities are scaled to be at the form $[kg/m^3]$. Both the rich MEG and lean MEG flow rates are given with water absorbed in the MEG.

All the mass flows for the species are made of the density of the rich MEG total flows or the lean MEG total flow combined with the total flow rate itself. In Equation (6.1) is an example of how the mass flow of the specie i are calculated. To calculate this mass flow the density for the specie in the rich MEG, ρ^i_{RM}, and the density of the rich MEG, ρ_{RM}, is used. These two variables are variables from Aspen Process Explorer that is not used in Matlab. The is the same approach to calculate the mass flow of the species in the lean MEG.

$$\dot{m}^i_{RM} = \frac{\dot{m}_{RM} \cdot \rho^i_{RM}}{\rho_{RM}} \tag{6.1}$$

In Equation (6.2), the calculation of the mass flow through the desalination plant is calculated. Because of strange data from the desalination plant, the desalination is set to be the mean value of the upwards and downwards mass flow,

instead of only the upwards mass flow. This is because sometimes the downwards mass flow is bigger than the upwards, which means that the desalination plant increases the mass in the MEG-recycler. This is not the case in the real process.

$$\dot{m}_{DES} = \frac{\dot{m}_{UP} + \dot{m}_{DWN}}{2} \tag{6.2}$$

The bypass mass flow, $\dot{m}_{BY}$, is not used in calculating the desalination mass flow.

6.1.1 Real production data sets

Due to many periods where the measurements in Aspen Process Explorer were incomplete, there was only obtained two data sets. But there was also some measurements in these two data sets that were incomplete.

The first data set is from 12. December 2012 until 12. January 2013. In this period there were some strange values in the measurements from the desalination process, which can indicate that the desalination process was either disabled or the data from it was corrupt.

The second data set is from 18. November 2012 until 17. December 2012. In this period there were some periods where both the mass flow of the rich MEG and the mass flow of the lean MEG, where about zero. This can be have forsaken by fault in the real system or faults in the measuring of the two states.

6.1.2 Filtering rich MEG total rate

The measurements for the rich MEG mass flow into the MEG-recycler is varying much. To prevent these big variations in the MEG-recycler, the mass flow of the rich MEG is filtered. This will lead to some errors in the amount of mass in the MEG-recycler, but this is not crucial because it is not of big importance that the state is very accurate, and it is not a physical real state.

The mass rate is filtered by taking the mean of the eleven values surrounding each value, the five on each side and the value itself. If the mean value is negative it is set to be zero. In Figure 6.1 the mass rate of the rich MEG is displayed before and after it is filtered.

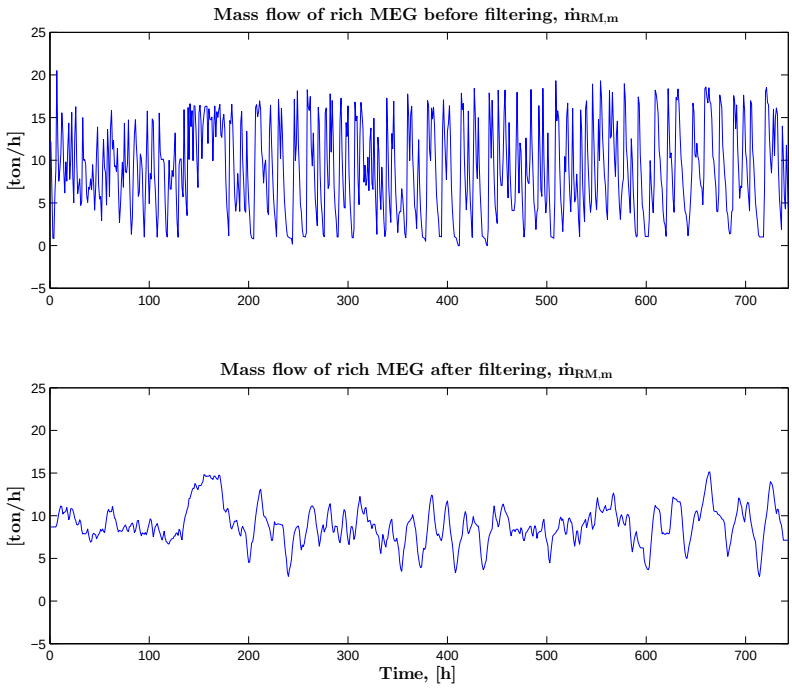

Figure 6.1: In the upper plot the mass flow of the rih MEG, before it is filtered, is shown. Below the result after the filtering is shown.

The total mass flow of rich MEG into the MEG-recycler still varies some, but it is varying less than before it was filtered. It was decided to not smooth it more, so the rich MEG mass flow should not lose too much of the variation in the signal.

6.2 Model and UKF implementation

In Table 6.2 the measurement, $\boldsymbol{y}$, and the input, $\boldsymbol{u}$, to the model is shown. The inputs consists of the total lean MEG mass flow, the total rich MEG mass flow, the input mass flow to the MEG-regenerator, the mass flow through the desalination plant and the mass flow of water removed from the MEG-regenerator. The measured states are all the mass flows of the species into the injection pipeline and out from the production line. The inputs to the model is not used as any states in model, while all the measurements are states in the model.

The states are all the states that are expressed in Chapter 3, Model development. The states that are measured are seen upon as the measured states of the model, while the states that are not measured are seen upon as the parameters of the system.

Table 6.2: The data used in Matlab.

Data	Variable	Type
Rich MEG total mass flow	$\dot{m}_{RM}$	$\boldsymbol{u}$
Lean MEG total mass flow	$\dot{m}_{LM}$	$\boldsymbol{u}$
Input mass flow	$\dot{m}_{IN}$	$\boldsymbol{u}$
Desalination mass flow	$\dot{m}_{DES}$	$\boldsymbol{u}$
Water removed	$\dot{m}_{OUT}$	$\boldsymbol{u}$
Rate of Mg^{2+} in rich MEG	$\dot{m}_{RM,Mg^{2+}}$	$\boldsymbol{y}$
Rate of Mg^{2+} in lean MEG	$\dot{m}_{LM,Mg^{2+}}$	$\boldsymbol{y}$
Rate of Ca^{2+} in rich MEG	$\dot{m}_{RM,Ca^{2+}}$	$\boldsymbol{y}$
Rate of Ca^{2+} in lean MEG	$\dot{m}_{LM,Ca^{2+}}$	$\boldsymbol{y}$
Rate of Sr^{2+} in rich MEG	$\dot{m}_{RM,Sr^{2+}}$	$\boldsymbol{y}$
Rate of Sr^{2+} in lean MEG	$\dot{m}_{LM,Sr^{2+}}$	$\boldsymbol{y}$

6.2.1 Initial values to the model parameters

From [5] it can be calculated that the Snøhvit reservoir was predicted to produce between 2.4 kg/h and 4.9 kg/h formation water, while the Albatross reservoir was predicted to produce between 1.4 kg/h and 2.0 kg/h formation water. This is data from 1999. For simplicity, and the fact that this is based on old and uncertain data, the Snøhvit reservoir is said to produces twice the amount of formation water than the Albatross reservoir.

The species used to identify the total formation water rate is shown in the table below. The chosen species are shown in Table 6.3 together with their expected concentrations. It is calculated with the density of formation water, ρ_{FW}, which is 1100 kg/m^3.

Table 6.3: The expected concentrations of each specie chosen to represent the formation water in the Snøhvit reservoir and the Albatross reservoir.

Species	Snøhvit	Albatross	α
Mg^{2+}	477 mg/l	2 369 mg/l	993
Ca^{2+}	4 628 mg/l	1 530 mg/l	306
Sr^{2+}	207 mg/l	321 mg/l	4490

The initial values for the mass rate of lean MEG and rich MEG for each species are set to the first value gotten from the measurements. The initial value is set for all the states for the rich MEG and lean MEG. The initial values for the species in the mass units are calculated from the equation for lean MEG out of the last mass unit. That means that the first calculated lean MEG mass rate for each specie into to injection pipeline will be identical with the measured value. The mass rate out of the first mass unit, with condensate water out and desalination, is set to be the difference between lean MEG mass rate and rich mass rate for each specie. The initial value set into the lean MEG pipeline for each specie, is also set as the initial

value for all the states in that pipeline. The same yields for the rich MEG pipeline. For the other states, initial values near what is expected is chosen.

Length of transport delays

The length of the transport delays in the production line and injection line is set to 12 hours and 72 hours respectively. This is done with respect to experiences that Statoil has from the field. This is also confirmed by measuring the transport delay in Aspen Process Explorer. In APE it is found that the transport delay varies around these proposed values.

The transport delay through the MEG-recycler is complicated to measure from the real system, since the MEG-recycle modeled in this model is not like the real MEG-recyler at Melkøya. Therefore the number of mass unit is set to between two and five by experience gained by different simulation. The number of mass units can also be used as a tuning parameter of the system.

6.2.2 Calculations of sigma points

The sigma points are calculated as shown in equations (5.17-5.18) and (5.24-5.25) in Section 5.2, the discrete unscented Kalman filter. The error covariance matrix is multiplied with the constant, n, to spread the sigma points in relation to the size of the system.

n represents the number of states in the system, and is typical 270+ states for this system. Many of the states are somehow similar to each other. Some of the states are identical, except that they yields for different species, and all the states used to model the transport delays are very similar to each other. Therefore the calculations of sigma points can be modified by replacing n with a smaller constant. This is done for several of the simulations of the system.

6.2.3 Constraints on states

The method described in Section 5.3, Constraints on the states, is implemented as a part of the unscented Kalman filter. This is done to prevent any of the states to become negative, since all the states are supposed to have nonnegative values. This has been done for some of the simulations of the system.

The method is set to check all the sigma points for negative values, and adjust their value to zero if that is the case. Then the model update of the states is done with the new sigma points. Further the sigma points that has been propagated by the state update is checked for negative values, and if their now has a negative value, the value is adjusted, as before, to zero.

6.2.4 Scaling of the states

To prevent large differences in the state values for the different states, the states are scaled to be "closer" to each other. Large differences in the states, and especially the large states in general, can lead to large variations in the error covariance

matrix. This can further make the error covariance matrix negative semi definite. When the error covariance matrix is not positive definite the unscented Kalman filter is unable to create it's sigma points. Before the scaling took place, it was especially the mass flow for each specie into the lean MEG pipeline, $\dot{m}^i_{LM,1}$ that caused the error covariance matrix to become negative semi definite.

The states are scaled to be in the range of approximately 0.01 to 5. That means that the mass flows for the species are scaled up. That is the mass rates in the lean MEG, $\dot{m}^i_{LM,k}$, the rich MEG, $\dot{m}^i_{RM,m}$, the mass rate out of the first mass unit, $\dot{m}^i_{OUT}$, the formation water, $\dot{m}^i_{FW}$, and the mass of each specie in the mass units, M^i_j. The total masses in the mass units, M_j, are scaled down.

The scaling has to take place when the initial values for the model is set before the simulation. In addition it has to be taken account for when the state model equation is updated and the measurement that consist of these scaled states has also to be scaled. Since all the measurements of the system is the lean and rich MEG mass rate out and into the MEG-recycler, respectively, all the measurement needs to be scaled.

6.2.5 Different frequency on measurement data

The measurements of the real process is taken with different frequency. The concentrations of species in the pipelines are taken rarer than the other used measurements, that are taken continuously. To take this into account the measurements that are taken rarely can be weighted more when there is a new measurement available, and taken out of the Kalman gain in those calculations for iterations where there are not any new measurements.

This is not implemented because there are small changes in the concentration of the species during the chosen data sets. And the flow rate of species in the pipelines, which are used as measurements in the Kalman filter, is also depending on the total mass flow of the lean or rich MEG.

Chapter 7

Tuning

In this Chapter the unscented Kalman filter will be tuned. The result of the tuning will be used when the Kalman filter is tested, which can be seen in Chapter 8, Results, later.

7.1 Tuning of the Kalman filter

The Kalman filter is mainly tuned by changing the noise matrices $\boldsymbol{Q}$ and $\boldsymbol{R}$ for respectively states, $\boldsymbol{x}$, and measurements, $\boldsymbol{y}$. The values in the matrices represents the expected deviation in the states/measurements, and also the uncertainty of these measurements/states. Small values in the tuning matrix means that there are small amount of noise, so the state or measurements are to be trusted. The matrices have only values on the diagonal, all other values are set to be zero.

The unscented Kalman filter can also be tuned by changing the initial value for the error covariance matrix $\boldsymbol{P_k^+}$. The tuning of the error covariance matrix is not prioritized since it is updated by the Kalman filter at each iteration. The tuning is performed with a real data series from 12. December 2012 until 12. January 2013.

The tuning was in some degree limited by the Kalman filter. If the values in the tuning matrices were too small or to large, the system was unable to perform the simulation. This was because the error covariance matrix would become negative semi definite, and the system would not be able to calculate the sigma points. This was especially seen for the state update noise matrix, $\boldsymbol{Q}$.

7.1.1 Tuning the measurements

The measurements are tuned by tweaking the measurements noise matrix $\boldsymbol{R}$. Because of the large oscillations on the measurements on the species in the rich MEG mass flow, and the smoothness of the measurements on the species in the lean MEG, the values associated to the lean MEG species are set smaller than for the rich MEG. The values that represent the measurements of the species in the lean MEG is set to be 0.1, while the values representing the measurements of the species

in the rich MEG are set to be eight times bigger, 0.8. The tuning values are shown in Table 7.1.

Table 7.1: Tuning parameters for the measurement noise matrix, $\boldsymbol{R}$. The shown values are the values on the diagonal of $\boldsymbol{R}$. The other values in the matrix are set to zero.

Measurement	Tuning values
$\dot{m}^i_{LM}$	0.1
$\dot{m}^i_{RM}$	0.8

7.1.2 Tuning the model updates

The tuning matrix for the state updates of the model, $\boldsymbol{Q}$, are tuned by a combination where two aspects are taken into account. The first aspect is how certain the different state updates are, the state updates are the equations that is contained in Section 9, Model discretization. The second aspect is to find tuning parameters that makes the system perform as expected. The last aspect is done by tweaking the parameters when simulating with real data, so the system would perform as wanted.

Initially all the tuning parameters were set to be 1. The parameters that was changed was the parameters associated with the calculation of the mass flow of each specie into the injection pipeline, Equation (4.10), which was changed from 1 to 5. The tuning parameters for calculating the mass flow of each specie in the formation water, Equation (4.16) were changed to 10. Further the parameters related to the expected value for the three species in the formation water, equations (4.18-4.20), were changed from 1 to 5. The last tuning parameters that were changed, were the parameters associated with the removed species from the MEG-recycler, equations (4.21-4.22). They were changed from 1 to 5. The tuning parameters for $\boldsymbol{Q}$ are shown in Table 7.2.

Table 7.2: Tuning parameters for the state update noise matrix, $\boldsymbol{Q}$. The shown values are the values on the diagonal of $\boldsymbol{Q}$. The other values in the matrix are set to zero.

State	Tuning values
M_i	1
M^i_i	1
$\dot{m}_{FW}$	1
$\dot{m}^i_{FW}$	10
$\dot{m}^i_{LM,1}$	5
$\dot{m}^i_{LM,j},\ for\ j > 1$	1
$\dot{m}^i_{RM}$	1
$\dot{m}^i_{OUT}$	5
α_i	5

As seen in this section and the section above, the tuning parameters of the $\boldsymbol{R}$ matrix are smaller than the values in the $\boldsymbol{Q}$ matrix. That indicates that the system relies, in general, more on the measurements than the state updates.

Chapter 8

Results

In this chapter the system will be tested for different scenarios. In the first section the model will be tested with test data. In the next section the system, including the model and the unscented Kalman filter will be simulated with test data. In the last section the system will be tested with real production data. In all sections it is performed one to three simulations.

8.1 Testing the model

The purpose of testing the model is to confirm that the essential dynamics of the model responds as expected. That is the time delays found in both the pipelines and in the MEG-recyler. In addition it is also important that the model will detect when formation water is produced from the reservoirs. Other important aspects are the desalination and the input and output mass flows to the MEG-recycler.

The three species, Mg^{2+}, Ca^{2+} and Sr^{2+}, is set to have an expected value of the total mass flow of the formation water. This is shown in Table 8.1 and means that specie 1 is expected to be $1/30$ of the total formation water mass flow. These are quite high and unrealistic values, but are chosen to make the results clearer and easier to comprehend. This yields for both the simulations of the model.

Table 8.1: The expected concentrations of each specie chosen to represent the formation water.

Species	Parameter	Value
Mg^{2+}	α_1	30
Ca^{2+}	α_2	15
Sr^{2+}	α_3	60

In this section it will be performed three simulations. The first case is to test the dynamics of the model when the well starts producing formation water. The

second case is to test the dynamics of the transport delays in the pipelines. The last case is to test the time delay in the MEG-regenerator.

8.1.1 Formation water

The formation water is added the system after a given period to see the response of the model. The formation water is added by setting a step in the three species. From the start there are a small amount of all three species in the MEG-recycler. These amounts will decrease because the species are removed as a part of the mass flow of removed condensate water out of the MEG-recycler.

The initial values of the system is shown in Table 8.2 together with the steps that are applied on the species in the formation water, $\dot{m}^i_{FW}$. The mass flows of the species in the pipelines are initially set to the value that the system would have if the process was in an equilibrium with the values given in the table.

The desalination plant is not used in this simulation. So all the species that are removed from the MEG-recycler, $\dot{m}^i_{OUT}$, is part of the mass flow of the removed condensate water out, $\dot{m}^i_{WAT}$.

Table 8.2: The initial values for the model together with the applied steps during the simulation.

Variable	Initial value	Values after 500 h
M_i	300000 kg	n/a
M^i_i	10 kg	n/a
$\dot{m}_{FW}$	0 kg/h	n/a
$\dot{m}_{IN}$	0 kg/h	0 kg/h
$\dot{m}_{DES}$	0 kg/h	0 kg/h
$\dot{m}_{LM}$	5000 kg/h	5000 kg/h
$\dot{m}_{RM}$	7000 kg/h	7000 kg/h
$\dot{m}_{WAT}$	2000 kg/h	2000 kg/h
$\dot{m}^1_{FW}$	0 kg/h	0.1 kg/h
$\dot{m}^2_{FW}$	0 kg/h	0.2 kg/h
$\dot{m}^3_{FW}$	0 kg/h	0.05 kg/h

The total mass rate of formation water is modeled by Equation (3.18) in Chapter 3. If the values for the species in the formation water are set to the values shown in Table 8.2, the total formation water rate should become 3 kg/h.

The transport delay was set to be three days, 72 hours, for the injection line and 12 hours for the production line. The MEG-recycler was modeled as four mass units. The time step were set to one hour and the duration of the simulation was 1500 hours.

The step is set to appear after 500 hours of simulation. This can be seen in the upper plot of Figure 8.1, the steps appear some hours after 500 hours because of the 12 hours transport delay in the production line. After the step the mass flow of specie 1 is still decreasing because of the removed water out of the MEG-recycler, that is because of the time delay in pipelines.

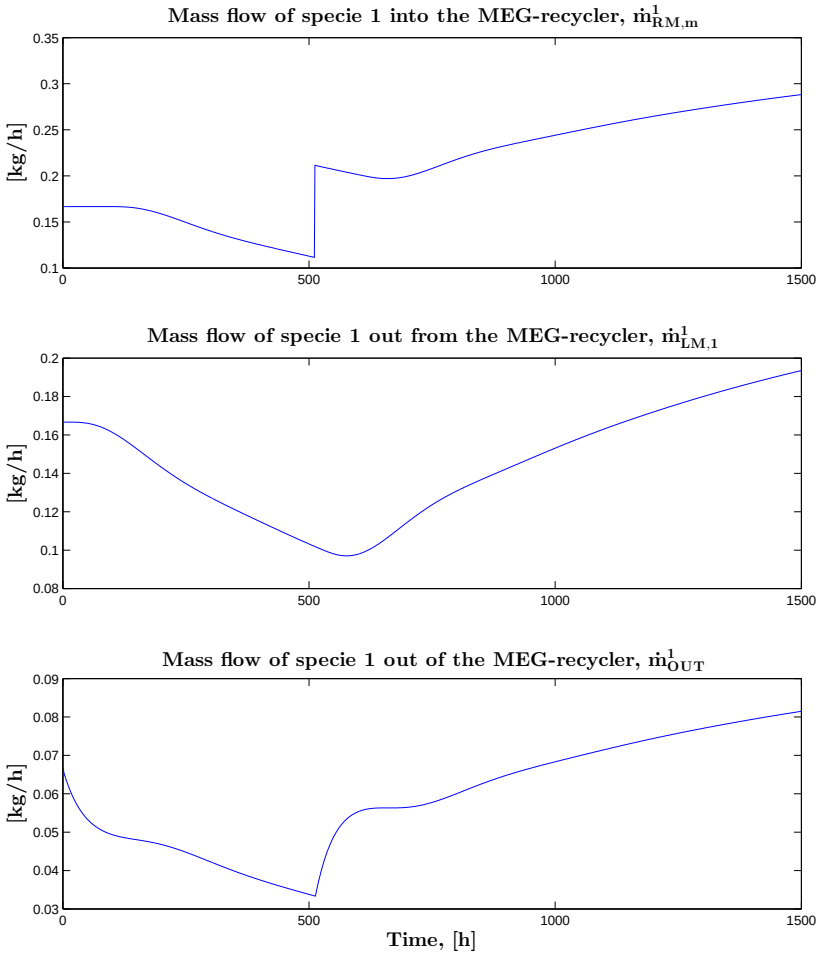

Figure 8.1: The response of mass flow into the MEG-recyler from the production line is shown in the upper plot. The response of the mass flow out of the MEG-recycler into the injection line is displayed in the middle plot. The bottom plot shows the mass flow of removed condensate water out from the MEG-recycler. All plots are for specie one, Mg^{2+}.

The transport delay in the pipelines leads to that the increased mass flows of the species out of the MEG-recycler takes a while before it reach the MEG-recycler again. When the extra species, caused by the production of formation water, reach the MEG-recycler after it has traveled through the whole MEG loop, the mass flow of the species in the rich MEG will start to increase. This can be seen in the upper

plot of Figure 8.1 after about 600 hours.

Since the water out mass flow is modeled to interfere with the first mass unit of the MEG-recycler, the response after the step is much more responsive in the bottom plot, displaying $\dot{m}^1_{OUT}$, than the middle plot, displaying $\dot{m}^1_{LM,1}$. It leads to that the mass flow out of the MEG-recycler is smoother than the mass flow into the MEG-recycler, $\dot{m}^1_{RM,m}$, displayed in the upper plot.

In the two upper plots it can be seen that the mass flows is constant at the beginning of the simulation. That is because the initial values of mass flow in the pipelines, and the initial mass in the mass units, are set as the same value in the whole pipeline and all the mass units respectively. Therefore it will take some time before the values are changed.

In Figure 8.2 the mass flow of the total formation water and the mass flow for specie one, Mg^{2+}, in the formation water is displayed at the top and bottom plot respectively. The step in value is seen at 500 hours for specie one. The change is also visible for the total formation water immediately. This is because it is modeled as a sum of the three species. This is shown in Equation 3.18 in chapter 3.

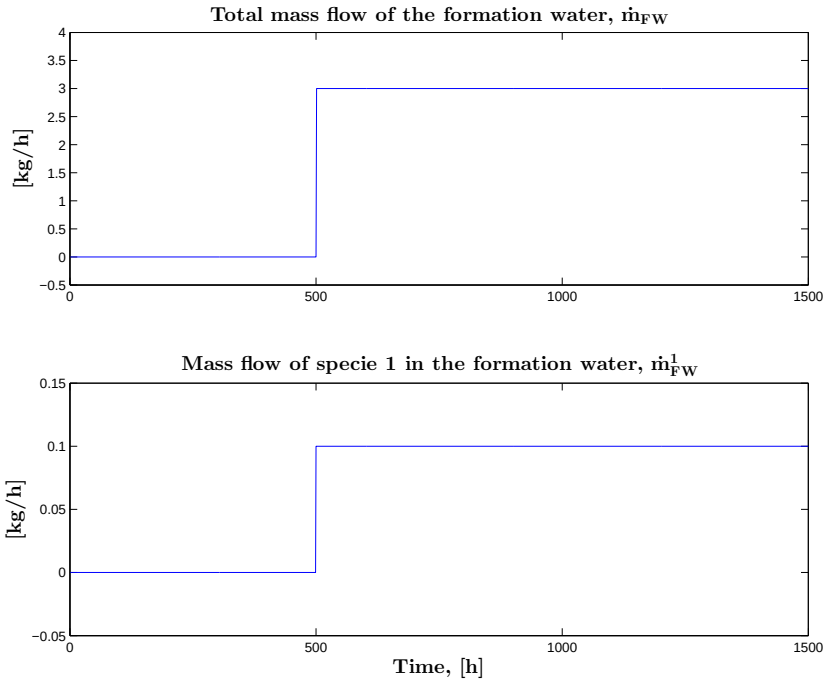

Figure 8.2: The upper plot shows the total mass flow of the formation water from the reservoir into the production line. The bottom plot displays the mass flow of specie one, Mg^{2+}, from the reservoirs into the production line. The bottom value is a part of the total formation water flow rate.

In Figure 8.3 the amount of the first specie is displayed for the first mass unit and the last mass unit of the MEG-recycler at the top plot and bottom plot respectively. The first mass unit is clearly more responsive than the last mass unit. This is mainly because the mass flow between the mass units are modeled as a stream with the same mass flow as the mass flow into the injection line, and the composition of the mass flow is equal with the composition of the mass unit as the mass flow is coming from. The mass flow rate of each specie between the mass units is therefore relatively small compared to the total amount of mass in the mass units.

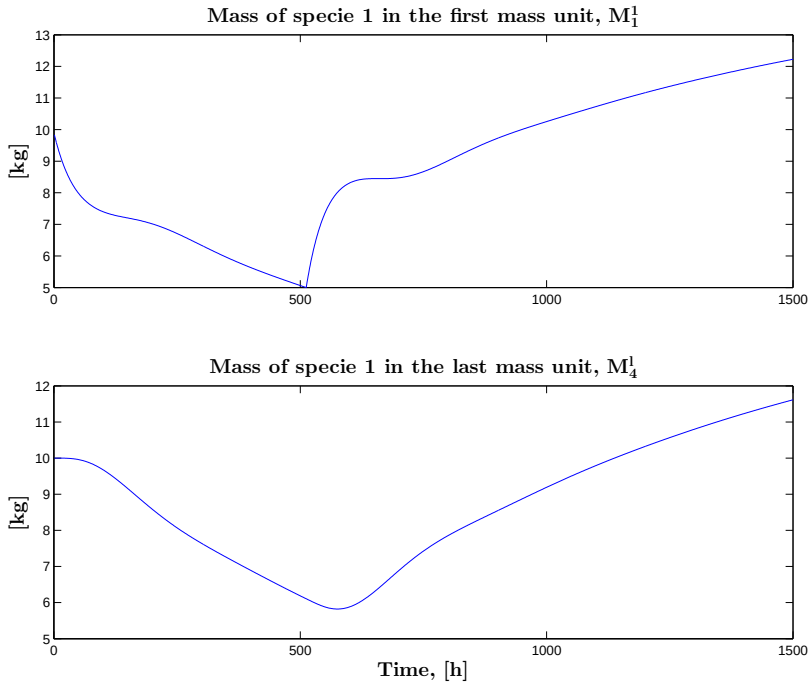

Figure 8.3: The mass of specie one, Mg^{2+}, in the first mass unit of the MEG-recycler, M_1^1, and in the last mass unit, M_4^1, is displayed in the upper and bottom plot respectively. The system is modeled with four mass units in this simulation.

It is desired that the last mass unit is as smooth as possible, since the mass rate of species out of the mass unit, $\dot{m}^i_{LM,1}$, is smooth. But it also has to respond at changes in the MEG-recycler.

8.1.2 Transport delay in the pipelines

The purpose of this simulation is to verify that the model takes into account the transport delays in the pipelines, and that the transport delays is at the correct size.

For this simulation the amount of each of the three species are increased with 500 kg in the first mass unit of the MEG-recycler. The values of the total amount of mass in the first tank is increased with 1500 kg. This is done after 500 hours of simulating and is done in the first mass unit of the MEG-recycler.

The initial values and the values applied after the step is shown in Table 8.3.

Table 8.3: The initial values for the model together with the applied steps during the simulation.

Variable	Initial value	Values after 100 h
M_1	300000 kg	+ 1500 kg
M_1^i	10 kg	+ 500 kg
$\dot{m}_{FW}$	0 kg/h	0 kg/h
$\dot{m}_{IN}$	0 kg/h	0 kg/h
$\dot{m}_{DES}$	0 kg/h	0 kg/h
$\dot{m}_{LM}$	5000 kg/h	5000 kg/h
$\dot{m}_{RM}$	7000 kg/h	7000 kg/h
$\dot{m}_{WAT}$	2000 kg/h	2000 kg/h

The transport delays are the same as the last simulation, 72 hours for the injection line and 12 hours for the production line. The number of mass units in the MEG-recycler is set to four during this simulation. The mass flow through the desalination is not active, and is therefore set to 0 kg/h. The simulation has a duration of 600 hours. In this simulation the mass flow of produced formation water is set to be zero.

In the upper plot the mass flow out of the MEG-recycler, $\dot{m}^1_{LM,1}$ and into the MEG-recycler, $\dot{m}^1_{RM,m}$, is plotted together. The transport delay is the combined transport delay for both pipeline, and is supposed to be 84 hours. This is verified, and can be seen on the plot.

In the bottom plot the mass flow of the first specie removed from the MEG-recycler is displayed. Since the desalination process is not in use during this simulation, the amount of removed mass is from the condensate water removed from the MEG-recycler. The rate which the specie is removed from the mass unit decrease rapidly and has a small upswing when the species have traveled around the whole MEG loop.

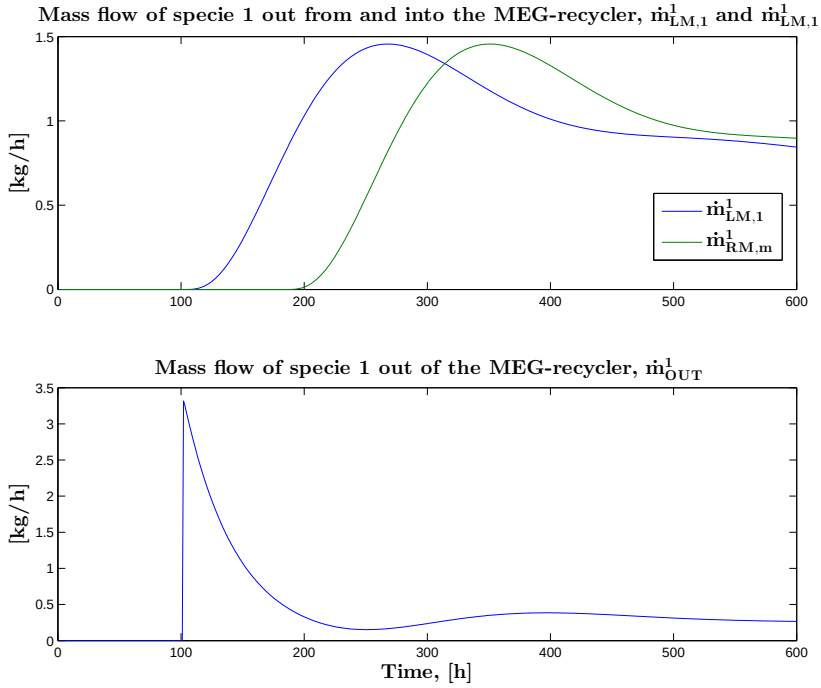

Figure 8.4: The response of mass flow into the MEG-recyler, together with the response of the mass flow out of the MEG-recycler, is shown in the upper plot. The bottom plot shows the mass flow removed from the MEG-recycler. All plots are for specie one, Mg^{2+}.

From Figure 8.4 it can be seen that the transport delay in the injection pipeline and the production pipeline works as expected and modeled. If the modeled transport delay in the pipelines is false, the transport delay can easily be adjusted by changing the number of states that represents the two pipelines.

8.1.3 Time delay in the MEG-recycler

The purpose of this simulation is to see the response on the last mass unit when there is a step in the first mass unit. The step is set to be an increase of 100 kg of the species in the first mass unit after 100 hours. The response is only shown for the first species, but the amount of the other species in the mass units behave in the same manner as the first specie. The values before and after the step is introduced, used in this simulation is the same as used in the section above. This is shown in Table 8.3.

Figure 8.5 displays the tank level for the first and last mass unit in the MEG-recycler. The MEG-recycler is modeled twice, first with three mass units and then

with four mass units. The results are combined together in the plot. The amount of specie 1 in the last mass units are clearly more smooth than the first mass unit. When the MEG-recycler consists of three mass units, the peak appears about 100 hours after the step. For the MEG-recycler the peak appear about 150 hours after the step, but the peak is smaller and smoother than the case is for the MEG-recycler with four mass units.

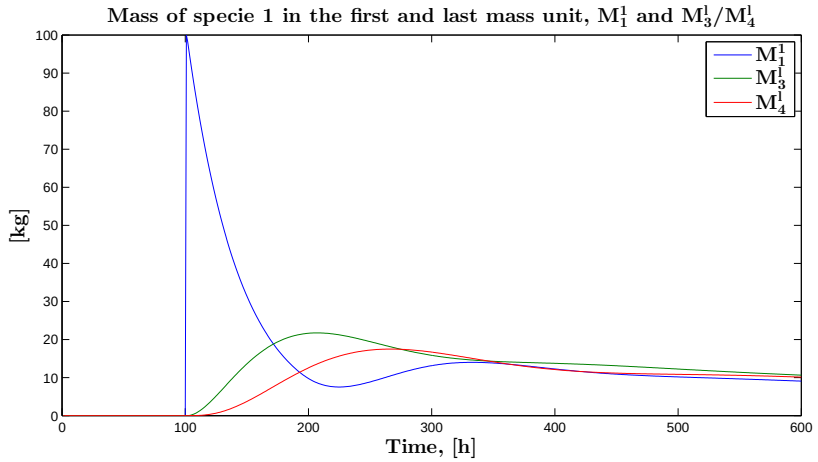

Figure 8.5: The mass of specie one, Mg^{2+}, in the first mass unit of the MEG-recycler, M_1^1, is shown with a blue line. The last mass unit, M_3^1 for the first simulation and M_4^1 for the second simulation, is displayed in the plot with a green and red line, respectively.

The most important property of the MEG-recycler is that the mass flow out from it is quite constant, and are not varying much. For three or four mass unit the value peaks at about 20 kg in the last mass unit. The change in the first mass unit is quite large step in mass, and therefore the response in the last mass unit maintains the expected response of the MEG-recycler. This yields for the mass unit modeled with both three and four mass units.

8.2 Testing the model with the unscented Kalman filter

The purpose of testing the system with both the unscented Kalman filter and the model together is to check if the Kalman filter will be able to predict incidents that the model itself is not able to detect.

Table 8.4: The expected concentrations of each specie chosen to represent the formation water.

Species	Parameter	Value
Mg^{2+}	α_1	3000
Ca^{2+}	α_2	1500
Sr^{2+}	α_3	6000

8.2.1 Detection of formation water

When the unscented Kalman filter is included in the simulation it can be tested if the system, the model and the Kalman filter, will detect the formation water. In this simulation the system starts in a steady state with none of the species in the system, not in the pipelines or in the MEG-recycler. When the formation water is extracted from the well, the result of it will be first be seen in the measurements taken of the content out of the production line, $\dot{m}^i_{RM,m}$. Therefore the increase of formation water will be simulated by changing the mass flow for the species into the MEG-recycler.

The tuning matrix for the state update, $\boldsymbol{Q}$, of the Kalman filter is not tuned for this simulation. The weight matrix is set to be the unit matrix, and the error covariance matrix is initial set to be the unit matrix. The measurement noise matrix is tuned as described in Chapter 7, Tuning. It is also proposed an alternative tuning, and the result is displayed in Figure 8.7.

The simulation is performed with constraints on the states and the spread of the sigma points are calculated with n adjusted to 100. These two methods are described in Chapter 6. The alternative method to calculate the removed specie from the MEG-recycler, the expression is expressed in Chapter 4.

After 200 hours a step is introduced in the measurements. The step will occur in the three species into the MEG-recycler and will simulate an increase in the production of formation water. The initial values and values after the step is displayed in Table 8.5. The measurement of the mass flows of the species into the lean MEG is increased as a ramp from 200 hours until 300 hours. The final value for all three specie is $6.25 \cdot 10^{-5}$ kg/h.

Table 8.5: The initial values for the model together with the applied steps during the simulation.

Variable	Initial value	Step values after 200 h
M_i	300000 kg	n/a
M_i^i	0 kg	n/a
$\dot{m}_{FW}$	0 kg/h	n/a
$\dot{m}_{IN}$	0 kg/h	0 kg/h
$\dot{m}_{DES}$	0 kg/h	0 kg/h
$\dot{m}_{LM}$	5000 kg/h	5000 kg/h
$\dot{m}_{RM}$	7000 kg/h	7000 kg/h
$\dot{m}_{OUT}$	2000 kg/h	2000 kg/h
$\dot{m}^1_{RM,m}$	0 kg/h	$6.35 \cdot 10^{-5}$ kg/h
$\dot{m}^2_{RM,m}$	0 kg/h	$6.3 \cdot 10^{-5}$ kg/h
$\dot{m}^3_{RM,m}$	0 kg/h	$6.45 \cdot 10^{-5}$ kg/h

The result of the simulation is shown for the first specie, Mg^{2+}. The response is the same for each of the two other species. In Figure 8.6 The response of the time step for mass flow into the MEG-recycler, the mass flow out of the MEG-recycler and the mass flow out of the desalination is displayed.

Before the lean MEG rate reach its final value, the rich MEG rate only reach about $2.5 \cdot 10^{-5}$ kg/h. When the lean MEG rate starts to increase, the rich MEG rate is able to reach its expected value. The estimated lean MEG rate follows the measured lean MEG rate very accurately.

The figure shows that the mass flow into the MEG-recycler, $\dot{m}^1_{RM,m}$, stabilizes at $6.35 \cdot 10^{-5}$ kg/h after the step. Further the flow out of the MEG-reycler stabilizes at about $6.25 \cdot 10^{-5}$ kg/h for the first specie. These are the expected values.

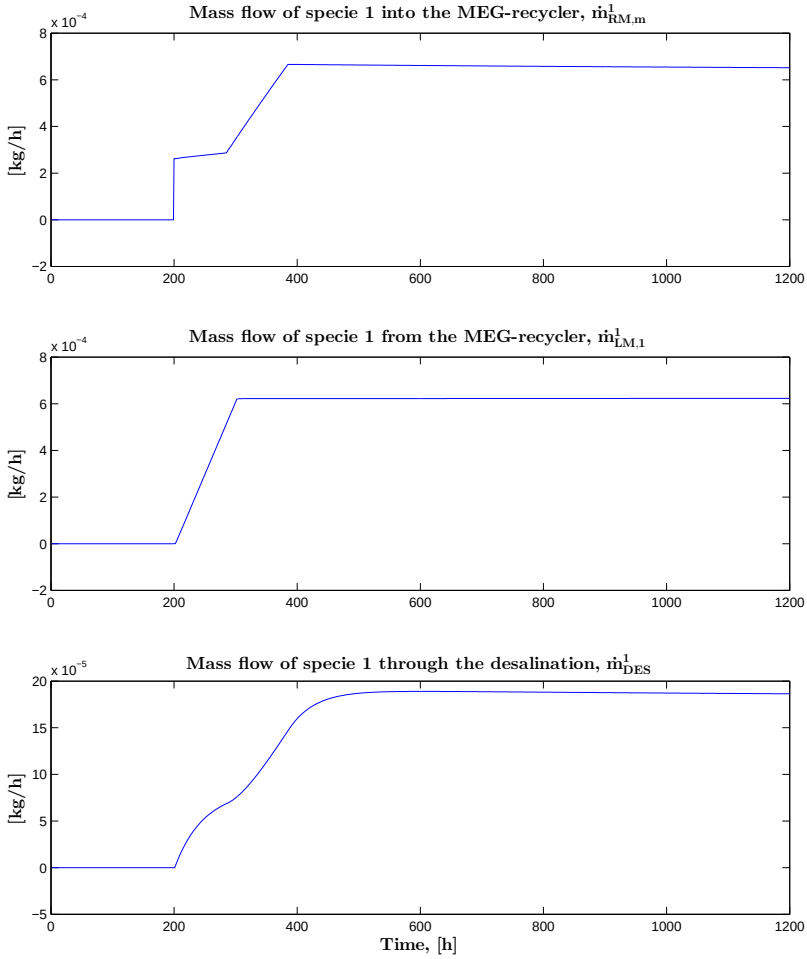

Figure 8.6: The response of mass flow into the MEG-recyler from the production line is shown in the upper plot. The response of the mass flow out of the MEG-recycler into the transportation line is displayed in the middle plot. The bottom plot shows the mass flow that is desalinated from the MEG-recycler. All plots are for specie one, Mg^{2+}.

From the Table 8.5 and 8.4 together with the calculation of the mass flow of formation water from Equation (4.17) it is expected that the produced formation water of this simulation will be 0.03 kg/h. For the First specie it is expected that the mass flow is $1 \cdot 10^{-5}$ kg/h.

In Figure 8.7 the mass flow of the produced formation water and for the first

specie is displayed. The response is shown for both the regular tuning of the measurement noise matrix, $\boldsymbol{R}$, and for an alternative tuning. The alternative tuning weights the measurements more than the regular tuning. The tuning matrix for the alternative is one tenth of the regular $\boldsymbol{R}$.

For both the tuning methods both the mass flows reach the expected value after the 3000 hours simulated. The predicted states use long time to reach their desired value. The alternative tuning reach the expected values before the regular tuning, but it has an over-swing that is more significant than for the regular tuning.

The slow response of the predicted mass flow rate of the produced formation water can be tolerated since the prediction of formation water has some uncertainties. The formation water is not expected to vary very much when produced either. Therefore the regular tuning is the preferred tuning of the measurement noise matrix.

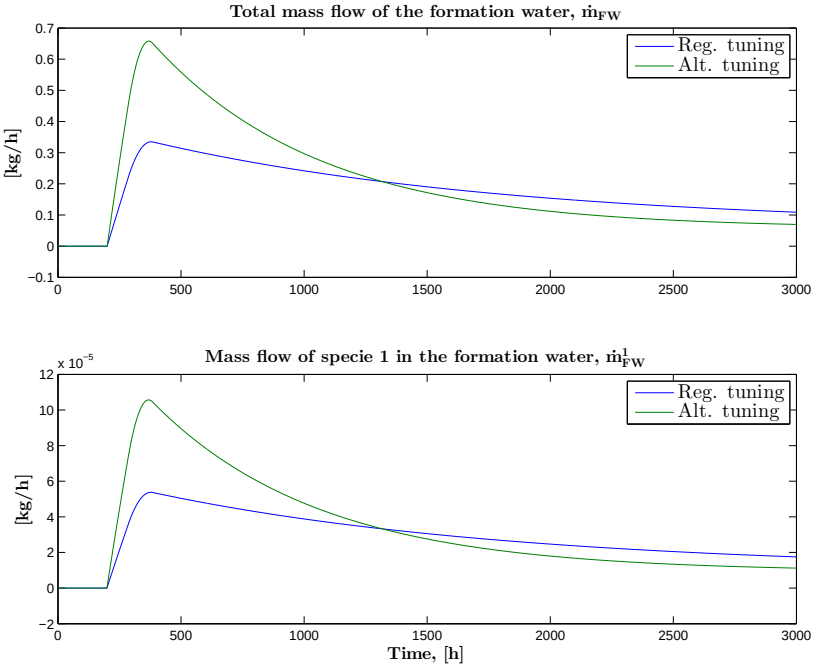

Figure 8.7: The upper plot shows the total mass flow of the formation water from the reservoir into the production line. The bottom plot displays the mass flow of specie one, Mg^{2+}, from the reservoirs into the production line. The bottom value is a part of the total formation water flow rate. The blue line shows the response with the regular tuning $\boldsymbol{R}_{reg}$, while the green line shows the response for the alternative tuning, $\boldsymbol{R}_{alt} = 0.1 \cdot \boldsymbol{R}_{reg}$.

Figure 8.8 displays the tank level for the first and second mass unit in the MEG-

recycler. In this simulation the MEG-recycler is modeled with two mass units. The last tank is less responsive than the first tank. The mass of specie out in the last tank continues to increase after the step has appeared. This is caused by the fact that the formation water uses long time before it is down at the right level.

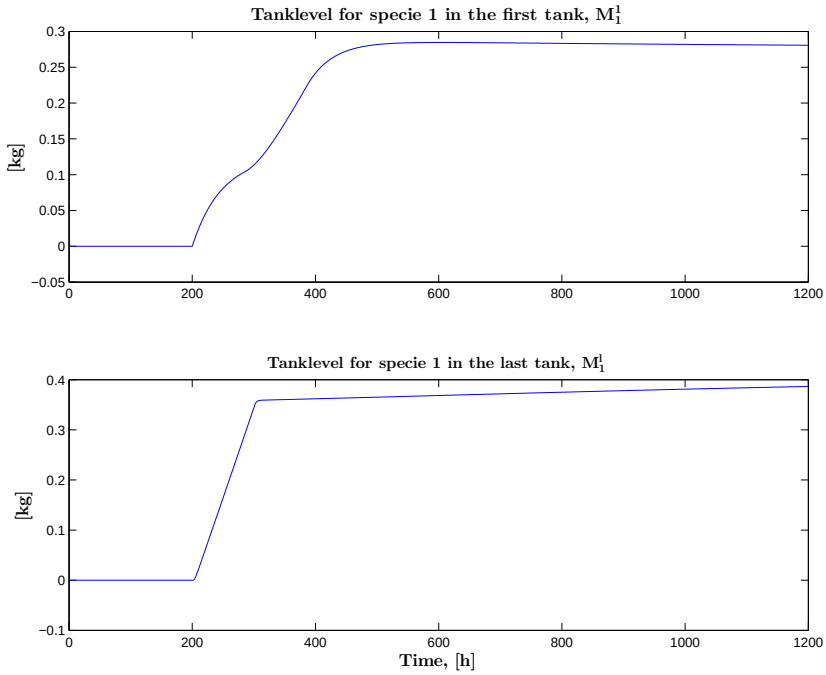

Figure 8.8: The mass of specie one, Mg^{2+}, in the first mass unit of the MEG-recycler, M_1^1, and in the last mass unit, M_4^1, is displayed in the upper and bottom plot respectively. The system is modeled with four mass units in this simulation.

8.3 Testing with real data

In this section the system, containing the model and the unscented Kalman filter, will be tested. The simulation is performed with real production data maintained from the Snøhvit field.

8.3.1 Testing the tuned Kalman filter

The purpose of this simulation is to test if the system, with the unscented Kalman filter, will work when real data is applied. It is also important to see how the system responds with the tuning parameters found in Chapter 7.

The system was tested without constraints on the states, since none of the states was in danger to become negative. The sigma points is made by replacing n with 100. This is done to make the system able to simulate. This was further discussed in Chapter 6, Model implementation. The contributions made from the expected formation water values, α_i, are set to zero. This is done in the Kalman gain, $\boldsymbol{K_k}$, for each iteration. It leads to that the expected formation water values are constant. They are set to the values found in Chapter 6.

In Figure 8.9 the mass flows in and out of the MEG-recycler is displayed. In the upper plot the the mass flow into the MEG-recycler are shown for the first specie in the rich MEG. The blue line is the state estimate, while the green line is measured value. The estimate follows the trend of the real value with a small time delay, but it do not varies as much as the real value. This is as expected because the model does not take into account the oscillations that exist on the rich MEG mass flow.

In the middle plot, the state estimate and the real measured value for the first specie in the lean MEG is displayed. The state estimate, in blue, almost follows the measurements, in green, perfect. This is the most important measurement to follow, since the rich MEG is also dependent on this mass flow. Since it follows that easy it means that there is enough slack in the model updates to be able to follow that measurement.

The last plot in Figure 8.11 is the removed mass rate of specie one from the MEG-recycler. The plot shows that this mass flow is almost unchanged. This is because the first method to predict the removed mass rate, Equation (4.21) is used.

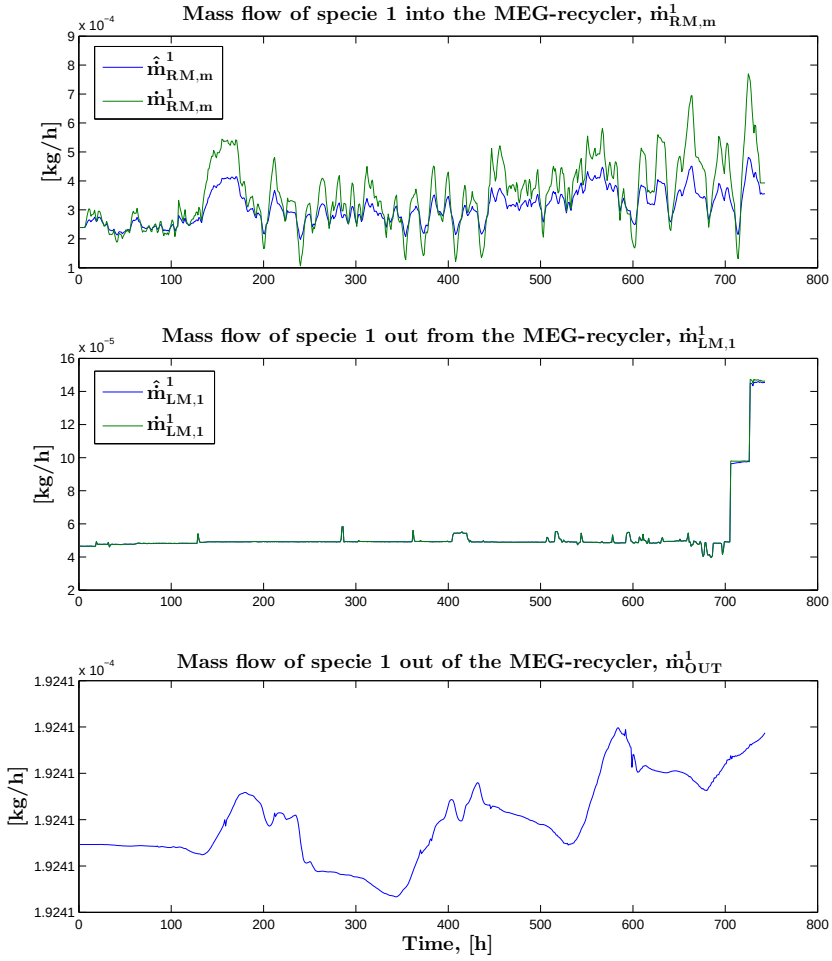

Figure 8.9: In the upper plot the mass flow of the first specie from the rich MEG pipeline is displayed. The middle plot shows the mass flow of specie one out of the MEG-recycler. The predicted value is shown with the blue line, while the measured value is shown with a green line. The bottom plot shows the removed mass rate of specie one out of the MEG-recycler.

In Figure 8.10 the total mass flow for formation water together with the mass flow of the first specie in the formation water is plotted. It can be seen that the total mass flow of formation water produced from the reservoirs is in the range 0.5 - 2.5 kg/h. As seen the total formation water do not solely follow the first specie, so the other species also influences the total mass flow. It is some variations in the

predicting of the produced formation water, which can indicate that the predicted value may vary a bit from the real value.

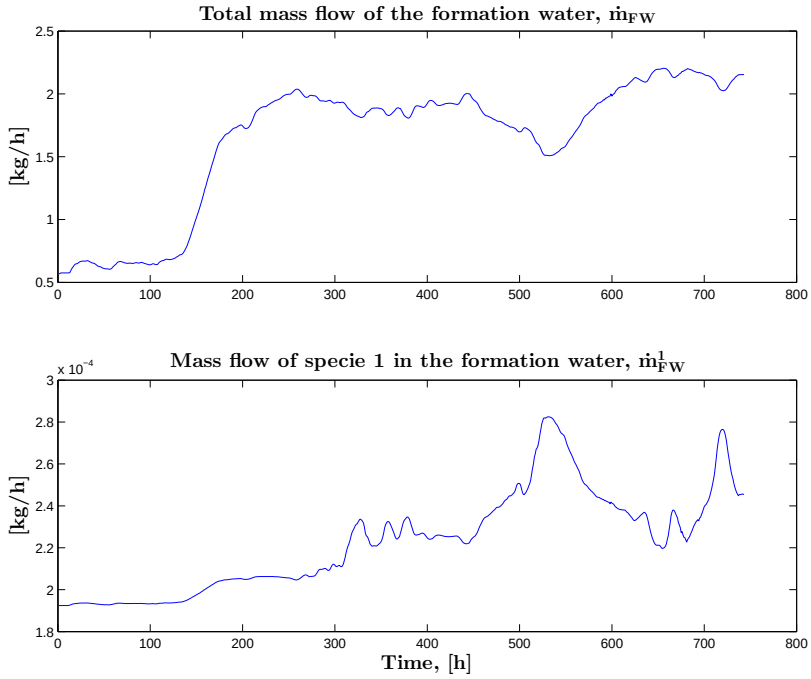

Figure 8.10: The upper plot displays the total mass flow of the produced formation water. And the bottom plot shows the mass flow of specie one in the produced formation water.

In Figure 8.11 the mass of specie one is displayed for the first (upper plot) and the last (bottom plot) mass unit. The amount of specie one in the last mass unit is very stable until the end of the simulation. In the last part, the amount of specie one in the last mass unit increases rapidly, this is to be able to send the rate of lean MEG that is shown in the middle plot of Figure 8.9. This shows that the Kalman is adapting the states, and not necessarily follows all the state updates given by the model. For this case it is not critical, since the amount of the species is not of interest. But it indicates that the model does not match the real system completely.

For the first tank there are quite large variations. This can indicate that the model is a part away from the real process.

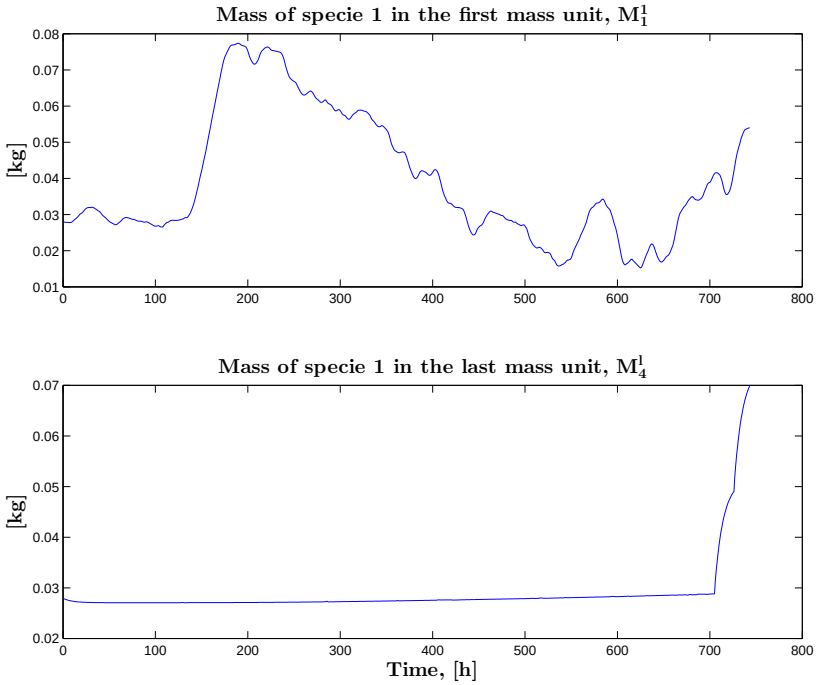

Figure 8.11: The upper plot shows the mass of the first specie in the first mas unit and the bottom plot shows the mass of the first specie in the last mass unit. The MEG-recycler is modeled as four mass units.

8.3.2 Unsuccessful simulations

When simulating the system with the other data set, the system is unable to simulate. That is caused by the error covariance matrix in the Kalman filter becomes negative semidefinite and the Kalman filter is unable to predict it's sigma points.

The data set is in some degree inconsistent, since the mass flow of the lean and rich MEG does not match the other data from the dataset. That indicates that the Kalman filter is not robust enough to handle data sets where there some inconsistence.

Chapter 9

Discussions

The simplified model of the process is proven to be a bit apart from the real process, but is somewhat adjusted by the unscented Kalman filter. Most of the difference is probably the oscillating mass flow of rich MEG into the MEG-generator, which is not taken into account in the model. The mass flow of removed species from the MEG-generator is also an element of uncertainty, because the mass flow through the desalination plant is not unambiguously from the production data. There are also done multiple simplifications with the MEG-regenerator.

When the system is able to simulate the system it is able to find a rate of produced formation water which is in the region of what is expected to be produced of formation water from Snøhvit. The spread of the sigma points in the Kalman filter has to be narrowed to be able to simulate, and the real process data can't be too inconsistent before the simulation fails. The data sets that the system is not able to simulate are data sets that are in some degree incomplete and has inconsistent data.

The system as it is now would probably have some periods when it is unable to operate it was to be used in real-time at the Snøhvit field. This is the same situation that Megsim experience at other location, where it is implemented, for Statoil. Since this system is solely focused on predict the produced formation water rate, the other system parameters are not as accurate as the current system, Megsim, is. The system established and implemented in this thesis should therefore be improved before it can be considered used by Statoil.

Chapter 10

Conclusion and further work

10.1 Conclusions

The simplified model is somewhat different from the real process at Snøhvit. The system is not robust enough to handle data from Snøhvit that are in some degree inconsistent or incomplete. When the system is able to perform it's predictions of the produced formation water, the rate of produced formation water predicted is in the region of what is expected at Snøhvit.

10.2 Further work

The further work is divided into proposals to improvements for the model and proposals of improvement of the Kalman filter.

10.2.1 The model

To make the model more like the real process at Snøhvit, there are some aspects that could be conducted. First of all the oscillations in the rich MEG rate into the MEG-regenerator can be taken into account in the model. This can be somewhat difficult to model, since the oscillations do not seem to be related to any of the other parts of the model.

Further the MEG-regenerator is modeled very simplistic in this model, and maybe a more advanced model of the MEG-regenerator will increase the model performance. The lean MEG rate out of the model can be considered to be modeled as a constant, instead of being dependent of the MEG-regenerator. It can lead to that the MEG-regenerator not being manipulated by the Kalman filter to fulfill the requirements of the lean MEG rate.

The modeled rate of species removed from the MEG-regenerator can possibly be modeled different. It was some uncertainties in the modeling of this parameter in this model.

The number of mass units in the MEG-regenerator, number of states in the lean MEG pipeline and number of states in the rich MEG pipeline can be further tuned if it found that the current numbers do not represent the real process ideal.

10.2.2 The Kalman filter

The Kalman filter can probably become more robust if the states are scaled even more equal each other than it is done in this thesis. It will lead to that the error covariance matrix is more probable to stay positive definite.

The frequency which the measurements are taken can be taken into account. This is explained in this thesis, but not taken into account in the simulations. In addition the system would become more robust it the measurements were taken more often than what is the case at Snøhvit.

Bibliography

[1] Statoil AS. Snøhvit, feb 2013. Availeble at http://www.statoil.com/en/OurOperations/ExplorationProd/ncs/snoehvit/Pages/default.aspx.

[2] R.G. Brown and P.Y.C. Hwang. *Introduction to random signals and applied Kalman filtering: with MATLAB exercises and solutions.* Number v. 1 in Introduction to Random Signals and Applied Kalman Filtering: With MATLAB Exercises and Solutions. Wiley, 1997.

[3] Water Population Department of Sustainability, Environment and Australien Government Communities. Ethylene glycol (1,2-ethanediol): Overview. Availeble at http://www.npi.gov.au/substances/ethylene-glycol/index.html.

[4] O. Egeland and J.T. Gravdahl. *Modeling and Simulation for Automatic Control.* Marine Cybernetics, 2002.

[5] L.A. Høyland, E. Herløe, O. Granli, and M. Hvidsten. Snøhvit - lng, technical design basis. 1999. Internal paper Statoil AS.

[6] G.P. Kojen. Megsim course_workshop sept 2011. 2011. Internal paper Statoil AS.

[7] MathWorks. Matlab overview. Availeble at http://www.mathworks.se/products/matlab/?s_cid=wiki_matlab_15.

[8] A.J. Mørk. Megsim vega - data reconciliation of ionic analysis data applied on the vega field, 2012.

[9] J. Nocedal and S.J. Wright. *Numerical optimization.* Springer series in operations research and financial engineering. Springer Science+Business Media, LLC., 2006.

[10] Store norske leksikon. Snøhvit, jun 2011. Availeble at http://snl.no/Sn%C3%B8hvit.

[11] Ministry of petroleum and energy. Norway's oil history in 5 minutes, june 2013. Availeble at http://www.regjeringen.no/en/dep/oed/Subject/oil-and-gas/norways-oil-history-in-5-minutes.html?id=440538.

[12] Oljedirektoratet. Snøhvit, may 2013. Availeble at http://factpages.npd.no /FactPages/default.aspx?nav1=field&nav2=PageView|All&nav3=2053062.

[13] L. Imsland R. Kandepu and B. A. Foss. Constrained state estimation using the unscented kalman filter. *16th Mediterranean Conference on Control and Automation*, 2008.

[14] D. Simon. *Optimal State Estimation: Kalman, H Infinity, and Nonlinear Approaches*. Wiley, 2006.

Appendix A

Notation and symbols

A.1 Notation

All matrices, $\boldsymbol{M}$, and vectors, $\boldsymbol{v}$, in this thesis is symboled with a bold font. Other parameters that are scalar, s, are written without any fonts. Matrices are written with capital letters, while scalars and vectors are mainly written with lower case letters. This is not the case for the mass in the MEG-regenerator, M, which is written with capital letters to easier distinguish them from the mass flows, $\dot{m}$.

A.2 Symbols

In Table A.1 the symbols used in this thesis are shown.

Table A.1: This table contains the different symbols used in this thesis.

Symbol	Description	Unit
$\dot{m}$	Mass flow	[kg/h]
M	Mass	[kg]
$wt\%$	Weight percent	[%]
ρ	Density	[kg/m^3]